SYNTHESIS AND CHARACTERIZATION OF
SPINEL FERRITE NANOPARTICLES

Submitted to the

Department of Physics

International Islamic University, Islamabad
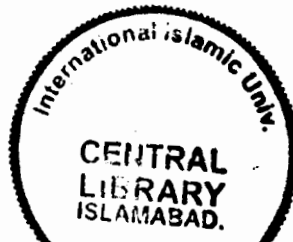
For the

MS degree

By

SAQIB RAHMAN

47-FBAS/MSPHY/F10

Supervisor

Dr. Kashif Nadeem

June 2012

Department of Physics
International Islamic University Islamabad

1. Electrical & Electronic Engineering
2. Magenetism & magnetic materials

ACCEPTANCE BY THE VIVA VOCE COMMITTEE

Title of Thesis: **SYNTHESIS AND CHARACTERIZATION OF SPINEL FERRITE NANOPARTICLES**

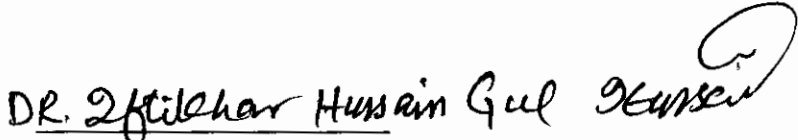**Name of Student:**   Saqib Rahman

Registration No.   47-FBAS/MSPHY/F10
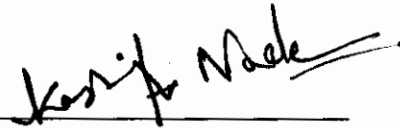
Accepted by the Department of Physics, Faculty of Basic & Applied Sciences, INTERNATIONAL ISLAMIC UNIVERSITY ISLAMABAD, in partial Fulfilment of the requirements for the Master of Science in Physics with specialization in superconductivity.
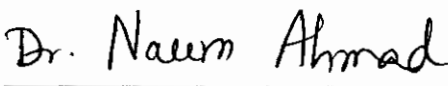
VIVA VOCE COMMITTEE

31·8·12

Dean

Chairman/Director/Head

DR. Iftikhar Hussain Gul

External Examiner

06/08/12

Research Supervisor

Dr. Naeem Ahmad

Internal Examiner

Acknowledgements

DECLERATION

I *Saqib Rahman* (47-FBAS/MSPHY/F10), student of MS in Physics (session 2010-2012), hereby declare that the matter printed in the thesis titled **"Synthesis and characterization of spinel ferrite nano-particles"** is my own work and has not been published or submitted as research work or thesis in any form in any other University or Institute in Pakistan or abroad.

Dated: _____

Signature of Deponent

Forwarding sheet by supervisor

The thesis entitled "**Synthesis and characterization of spinel ferrite nano-particles**" submitted by Mr. Saqib Rahman in partial fulfillment of MS degree in Physics has been completed under my guidance and supervision. I am satisfied with the quality of student's research work and allow him to submit this thesis for further process to graduate with Master of Science Degree from Department of Physics, as per IIU rules & regulation.

Date: _____

Dr. Kashif Nadeem

Assistant Professor
Department of Physics
International Islamic University
Islamabad.

CONTENTS   Title Page

List of Tables

List of Figures

Abstract

Soft magnetic spinel ferrite Zn-Mg ferrite ($Zn_{1-x}Mg_xFe_2O_4$, where x = 0.0 – 0.5 nano-particles have been synthesized by co-precipitation method. Structural characterization includes X-ray diffraction (XRD), scanning electron microscope (SEM) and Fourier transform infrared (FTIR) spectroscopy. Magnetic characterization was done by using vibrating sample magnetometer (VSM). The average particle size lies in the range 29–60 nm for different compositions. All the XRD intensity peaks reveal the spinel structure of these nano-particles. FTIR spectroscopy shows the characteristic absorption bands of spinel ferrite nano-particles at 420 cm^{-1} and 545 cm^{-1}. The band at 545 cm^{-1} shows a monotonic increase with increasing Mg concentration. Magnetization shows an increasing trend with increasing Mg concentration which is due to the rearrangement of cations at tetrahedral and octahedral sites, while the coercivity shows a small change on increasing Mg concentration due to the soft nature of the ferrite composition $Zn_{1-x}Mg_xFe_2O_4$. All these measurements show the successful synthesis of $Zn_{1-x}Mg_xFe_2O_4$ nano-particles with enhanced magnetic properties which can be best alternatives to other toxic soft magnetic materials such as NiZn ferrite ($Ni_{1-x}Zn_xFe_2O_4$) nano-particles.

CHAPTER – 1
Nanotechnology

1.1   Introduction

Nanotechnology can be defined as the study and use of structures having one dimension between 1 – 100 nm. Micro engineering is the science of engineering that deals with particle manipulation if those particles are smaller than 100 nm. Simply we can say "engineering with atomic precision" [1].

According to the old definition "the production characterization, design and application of materials, systems and devices by controlling size and shape of the nano-scale itself considered to cover the range from 1 to 100 nm" [2]. A little different concept is given by "controlled and deliberated, manipulation, modeling measurement, precision placement and production of matter at the nano-scale in order to create devices, materials and systems with fundamentally new properties and functions" [2].

It is simple to understand that the properties of a single atom are different from a bulk material. A single metal atom is non-conducting and bulk metal is conducting, so the question is what should be least size limit that still keeps its "bulk" properties. Typical dimensions where properties become highly size dependent is between 1 nm and 100 nm. The materials may have amazing properties in case of 1-D, 2-D, and 3-D of a material lie in the nano-meter regime. These properties are very dissimilar from that of the bulk materials [3]. Switching from micro particles to nano-particles leads to many changes in physical properties.

High surface to volume ratio plays a key role in these changes and it becomes more significant as the size of the particles decreases to nano-meter regime. The ratio of surface area to volume increases significantly as the size falls below 50 nm with particles becoming exponentially more proficient as creating surface area. Approximately a 4 nm zinc particle has 60% atoms on the surface, a 15 nm particle has 25% atoms on the surface, and a 40 nm particle has only 3% of its atoms on the surface [4]. Similarly

magnetic materials such as Ni, Co, Fe, Fe_3O_4, etc. magnetic properties are dependent on the size of particle. The magnetic memory or 'coercive force' is dependent on size [4].

Physics is different on the scale of nano-meter. In nanotechnology one has to work with individual molecules and atoms rather than working with bulk materials. By controlling the composition and structure of materials and devices at nano-size, new functionality can be developed and the performance of the products can be greatly enhanced.

Over the past few decades, nano-structure materials have been the source of great interest, with the potential for widespread industrials, electronic and biomedical applications [2]. These applications include polymeric materials, ceramics, and metals. Nano-materials have in fact been synthesized and used by humans for hundreds of years e.g. the red color of some stained glass and the ruby are due to gold nano-particles trapped in some glass matrix [2].

Nano-crystalline materials are basically polycrystalline with grain sizes in the range 1-100 nm that are found to show increased ductility and toughness, improved hardness, optoelectronic and superior magnetic properties [5]. Nano-crystals are actually collection of atoms that merge into a crystalline form of matter that can be defined as a 'cluster'. Usually around 10-15 nm in diameter, nano-crystals are bigger than molecules but less significant than bulk solids and therefore often shows chemical and physical properties somewhere in-between.

The reason for this behavior is the high dispersety of nano-crystalline systems. Properties, which are generally determined by the molecular structure of the bulk lattice, now become more dominated by the surface defects. Nanotechnology is truly a multidisciplinary area of research, improvement and development, bringing together the disciplines of biology, chemistry, engineering and medicine. As it unites variety of fields, it is quite an alluring and challenging branch of science. The recent significance in nano-structures results from their various potential applications such as in material development, electronics, biomedical sciences, magnetism, optics, energy storage and electrochemistry. Chemistry involves in preparation methods, physics involves in

investigation methods and biology involves in wide range of functional molecules contribute all together to the great development of the field.

1.2   Concept of Magnetism

Magnetism can be defined as the force of attraction or repulsion of a magnetic material due to the arrangement of its atoms, predominantly its electrons.

The magnetization of a material can be defined in terms of density of net magnetic dipole moments m in the material. We describe a vector quantity known as the magnetization,

$$M = \mu_{total} / V \dots\dots\dots\dots\dots\dots\dots\dots\dots\dots\dots\dots\dots \quad (1.1)$$

Where μ_{total} is net magnetic dipole moment and V is volume.

The total magnetic field B in the material is express by,

$$B = B_o + \mu_o M \dots\dots\dots\dots\dots\dots\dots\dots\dots\dots\dots\dots \quad (1.2)$$

Where μ_0 is the magnetic permeability of free space and B_0 is the external applied magnetic field.

A different method to view the magnetic fields that arise from magnetization of materials is to define a quantity known as magnetic field strength H. In term of magnetization M, B may be expressed as,

$$H = B_o / \mu_o = B / \mu_o - M \dots\dots\dots\dots\dots\dots\dots\dots \quad (1.3)$$

$$B = \mu_o (M + H) \dots\dots\dots\dots\dots\dots\dots\dots\dots\dots \quad (1.4)$$

M and H both have the similar units, amperes/meter.

$$B = \mu_r \mu_0 H \dots\dots\dots\dots\dots\dots\dots\dots\dots\dots\dots\dots \quad (1.5)$$

Where

$$\mu_r = (1 + M / H) \dots\dots\dots\dots\dots\dots\dots\dots\dots\dots \quad (1.6)$$

1.2.2 <u>Magnetic Susceptibility and Permeability</u>

The magnetic susceptibility describes the degree (and sense) of magnetization given an applied field strength. It is characteristic of the substance and it is highly temperature dependent.

$$M = \chi H \dots\dots\dots\dots\dots\dots\dots\dots\dots\dots\dots\dots\dots\dots (1.7)$$

The expression for the total magnetic field can be rewritten as,

$$B = \mu_m H \dots\dots\dots\dots\dots\dots\dots\dots\dots\dots\dots\dots\dots (1.8)$$

Where

$$\mu_m = \mu_o(1 + \chi) \dots\dots\dots\dots\dots\dots\dots\dots\dots\dots\dots (1.9)$$

1.3 Magnetic Properties of Solids

Materials can be categorized by suitable measurements in different types such as:

- diamagnetic,

- paramagnetic,

- ferromagnetic,

- antiferromagnetic,

- ferrimagnetic,

All are depending on their behaviour to an external applied magnetic field.

1.3.1 <u>Diamagnetism</u>

When a material is positioned in a magnetic field, the magnetic dipole moments appear opposite to direction of external field. Diamagnetism is exhibited by those elements which have paired electrons. Such types of materials have negative and small

value of susceptibilities. The diamagnetic effect in materials can be observed only if the paramagnetic or the ferromagnetic effect does not mask the weak diamagnetic effect.

Diamagnetism is a feeble type of magnetism which can be observed in the presence of external applied magnetic field. The direction of induced magnetic moment is opposite to that of the applied field.

Diamagnetic materials are generally attracted towards the weak magnetic field regions, when positioned between the poles of a strong electromagnet.

1.3.2 **Paramagnetism**

All molecules and atoms with unpaired electrons show paramagnetic effects; e.g. compounds of transition metals with ions having unfilled electron shell, free radicals, free atoms [6]. In paramagnetic materials, there is no cancellation of moment of electron so there is net magnetic moment in the atom. Without the presences of applied field, atomic magnetic moments are randomly aligned and cancelled the magnetization effect of one another. These net magnetic moments can be positioned in the direction of the applied field [6]. They consequently have a small but positive susceptibility and a relative permeability somewhat in excess of one. It can be observed in metals as a consequence of the magnetic moments linked with the spins of the conducting electrons [6].

Paramagnetic materials repel and attract like normal magnets when placed in a magnetic field. Paramagnetic materials are magnetic in nature as long as the external field is present. The magnetization is lost when the magnetic field is removed .paramagnetic materials always obey Curie's Law:

$$M = C.B / T \dots\dots\dots\dots\dots\dots\dots\dots\dots\dots\dots\dots\dots\dots\dots (1.10)$$

This law implies that paramagnetic materials show tendency to become more and more magnetic due to increase in applied magnetic field, but become less magnetic with the increase in temperature. Generally paramagnetic effects are weak (magnetic susceptibility of the order of $\chi_m \sim 10^{-03}$ to 10^{-05}.

Ferromagnetic materials become paramagnetic above the Curie temperature. Calcium, Liquid Oxygen, Platinum, Strontium, Uranium, Aluminum, Barium, are some paramagnetic materials.

1.3.3 **Ferromagnetism**

Ferromagnetic materials show spontaneous magnetization when external magnetic field is not present. The atomic magnetic moments are aligned even in the absence of applied magnetic field. This indicates that there is a strong internal field with in materials that makes the atomic magnetic moments aligned with earth other [7].

Ferromagnetism is one of the strongest types of magnetism in which a material can show a spontaneous magnetization. Most of the magnetic behavior that we experience in routine life is based on ferromagnetism. Such materials include nickel, iron and cobalt. Ferromagnetic material becomes paramagnetic above certain critical temperature called Curie temperature T_c.

1.3.4 **Anti-Ferromagnetism**

This is the phenomenon in which materials have strong tendency toward an anti-parallel alignment of magnetic moments in the absence of external magnetic field. These are such type of materials in which there is an anti-parallel alignment of spins in two interpenetrating structures as a result that there is no net bulk spontaneous magnetization.

For ferromagnetic materials, it is vigorously suitable for the spinning atom to align, thus give rise to spontaneous magnetization. On the other hand in anti-ferromagnetic materials, it is vigorously favorable for the spins to oppose, leading to no net magnetization. Therefore it is the opposite of ferromagnetism. Usually, anti-ferromagnetic materials reveal anti-ferromagnetism at low temperature, and become disordered above a particular temperature; the transition temperature is known as the Neel temperature. The material is normally paramagnetic above that temperature. The anti-ferromagnetic behavior at low temperature generally induces diamagnetic properties,

but can sometimes show ferromagnetic behavior, which in many physically observable properties are more analogous to ferromagnetic interactions. As the temperature is decreased, the magnetic susceptibility " χ_m " of an anti-ferromagnetic material will become maximum; on other side paramagnet will continually increase with decreasing temperature [6]. The relative permeability and susceptibility for all these materials are are shown in Table 1.1.

Table 1.1 Comparisons between Diamagnetic, paramagnetic and ferromagnetic of magnetic induction, relative permeability and susceptibility.

Type	Magnetic Induction (B)	Relative Permeability (μ_r)	Susceptibility (χ_m)
Diamagnetic	small, opposite H	<1 (barely, so $\mu \approx \mu_o^-$)	Negative, -10^{-5}
Paramagnetic	small, with H	>1 (this time $\mu \approx \mu_o^+$)	Positive, 10^{-5} to 10^{-6}
Ferromagnetic	large, with H	>>1	>>1

1.3.5 Ferrimagnetism

Ferrimagnetic substances show a similar behavior as the ferromagnetic substances but have an anti-parallel alignment of the magnetic moments as in the case of anti-ferromagnetism with the difference that they do not cancel each other. Net magnetic moment in the absence of an external magnetic field is due to the difference in spin magnitude. The susceptibility, magnetic behavior and magnetic moment ordering for all these materials are shown in Table (1.1-1.2).
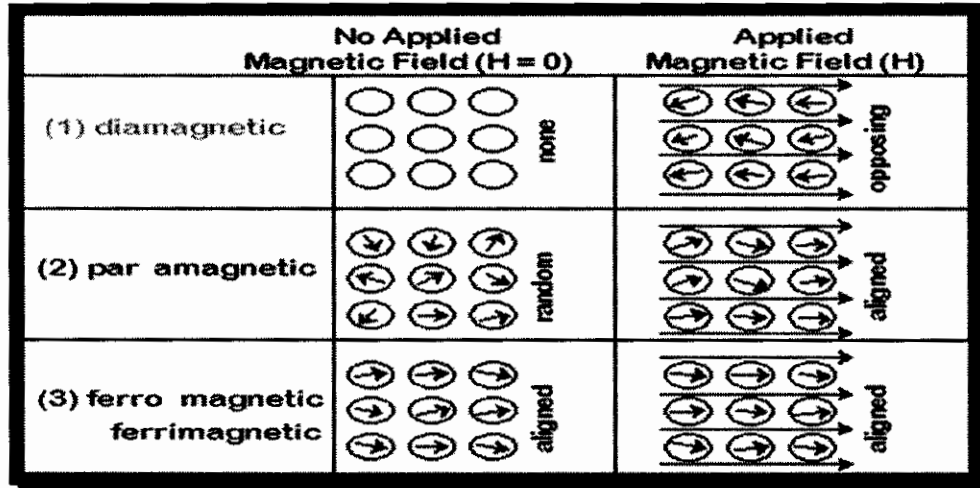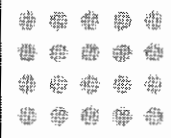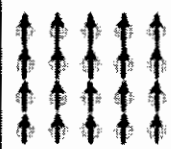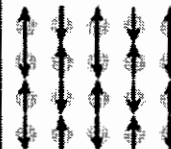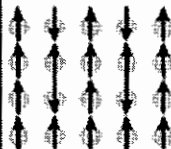
Fig. 1.1 Magnetic moment ordering and alignments [8].

Table 1.2 Summary of magnetism [8].

Type of Magnetism	Susceptibility	Atomic / Magnetic Behaviour		Example / Susceptibility	
Diamagnetism	Small & negative.	Atoms have no magnetic moment		Au Cu	-2.74x10^{-6} -0.77x10^{-6}
Paramagnetism	Small & positive.	Atoms have randomly oriented magnetic moments		β-Sn Pt Mn	0.19x10^{-6} 21.04x10^{-6} 66.10x10^{-6}
Ferromagnetism	Large & positive, function of applied field, microstructure dependent.	Atoms have parallel aligned magnetic moments		Fe	~100,000
Antiferromagnetism	Small & positive.	Atoms have mixed parallel and anti-parallel aligned magnetic moments		Cr	3.6x10^{-6}
Ferrimagnetism	Large & positive, function of applied field, microstructure dependent	Atoms have anti-parallel aligned magnetic moments		Ba ferrite	~3

1.4 Ferrites

Ferrites are basically ceramic materials and general formula of ferrites is MFe_2O_3, where M is divalent elements that are Co, Fe, Ni, Mn, and Zn. The old and famous ferrite is magnetite (Fe_3O_4), which can be think about a double oxide containing ferrous and ferric oxides $(FeO \cdot Fe_2O_3)$. Intermediate ferrites can be prepared in which the divalent cation may be a combination of ions, e.g.: $Mg_{1-x}Mn_xFe_2O_4$ and $Zn_{1-x}Mg_xFe_2O_4$, consequently that a wide range of magnetic properties and composition are existing. These, along with the Ba and Sr ferrites, form the mainstream for electronic applications of magnetism .Generally ferrites have most important and interesting magnetic properties. These are magnetic materials that show a series of magnetic and electrical properties which are very useful for a large variety of technological applications.

The technical applications of ferrites based on the combination of intrinsic properties that is saturation magnetization, Curie temperature, microstructure, grain size, porosity, etc. Commercially important and well-known ferrites should possess high purity, chemical homogeneity, fine grain size and high density.

1.5 Soft Ferrites

Soft ferrite materials show ferromagnetic behavior. Soft ferrite nano-particles mean that the nano-particle magnetization can reverse direction without dissipating large amount energy. In soft ferrites there are two sets of unpaired inner electron spin moments in opposite directions that produces net magnetic moment.(these electron spin moments do not cancel each other due to opposite direction) Ferrites can be used electromagnetic cores contain nickel, zinc or manganese compounds can also be used in transformer. Soft ferrites have low coercivity. They have a low coercivity and are called soft ferrites. Soft magnetic ferrites are major materials for compact switch mode power supplies. They have many applications and used in computer memories and high frequency transformer

cores. Computer hard disks, floppy disks, credit cards and video cassettes are some of very common soft ferrite devices [9].

1.6 Hard Ferrites

In oppositely, permanent ferrite magnets are called "hard ferrites", which have a high value of remanence after magnetization, are composed of barium and iron or strontium oxides. Hard ferrites nano-particles are those which are highly resistant to become demagnetized, a necessary characteristic for a permanent magnet. Hard ferrites generally used in many applications such as generator, relay, motors, loud speakers, telephones etc. Hard ferrites are the most commonly used magnets in radios.

1.7 Types of Ferrites

Ferrites can be classified in to three different types.
1.   Spinel ferrites

2.   Hexagonal ferrites

3.   Garnets

We will discuss only spinel ferrite here which is of our interest in this thesis.

1.7.1 <u>Spinel Ferrites</u>

The spinel ferrites commonly known as cubic ferrites are the most widely used ferrites. At microwave frequencies low eddy current losses and high value of electric resistivity make them ideal for their use. The spinel structure was initially determined by Nishikawa and Bragg in 1915. The spinel lattice consists of a close packed oxygen arrangement where 32 oxygen ions form a unit cell. MFe_2O_4 is the chemical composition of a spinel ferrite. Where M is the divalent metal ion that is, Mg^{2+}, Co^{2+}, Zn^{2+}, Fe^{2+}, Ni^{2+}, and Cd^{2+}.

Spinels crystal structure is basically cubic; with the oxygen ions forming an FCC lattice having eight formula units per cell in structure of spinel. The unit cell of spinel carry 32 oxygen ions. The formula can be written as $M_8Fe_{16}O_{32}$. Within these lattices there occur two types of interstitial positions and which can be filled by the metallic cations. In a unit cell, there are 32 octahedral (B) sites and 64 are tetrahedral (A) sites.

1.7.1.1   Tetrahedral Sites

In spinel ferrites the interstitial sites are called (A) sites and these are surrounded by or coordinated with four closest adjacent oxygen ions whose lines linking their centers form a tetrahedron. Thus (A) sites are said tetrahedral sites. Three atoms coincide one another are in plane; the fourth atom sites in the symmetrical position on top. For charge balance of the system just 8 tetrahedral (A) sites out of 64 sites are occupied. In a FCC there are 8 tetrahedral (A) sites per unit cell. Figure 1.2 shows the tetrahedral location in the FCC lattice.
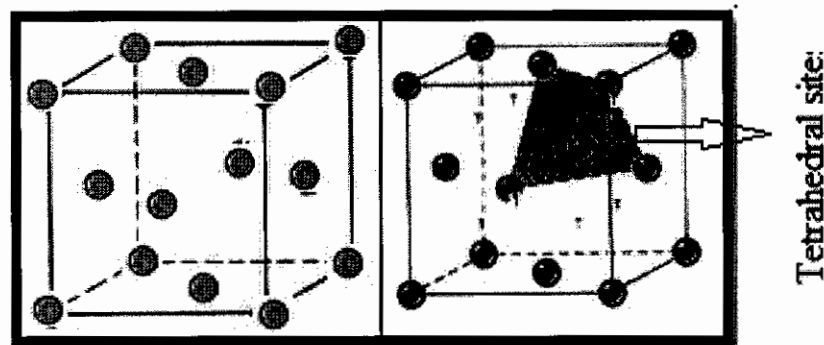
Fig. 1.2 Tetrahedral sites in FCC lattice.

1.7.1.2 Octahedral Sites

Second type of site is (B) site and these types of sites are called octahedral sites. These sites are synchronized by six adjacent neighbor oxygen ions whose center linking lines describe an octahedron which are named octahedral (B) site. In an octahedral (B)

site the interstitial is in the middle of an octahedral pattern by 6 lattice atoms. Four regular atoms are located in a plane and the other two are in asymmetrical location just above or below. Spinel structure has 32 octahedral sites but for charge neutrality 16 octahedral (B) sites are occupied. In a FCC there are four octahedral sites (B) per unit cell. Figure 1.4 indicates octahedral site in an FCC lattice.
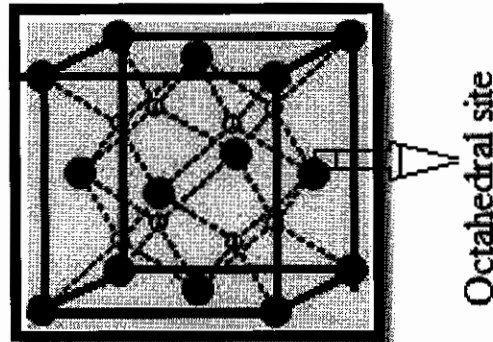
Fig. 1.3 Octahedral sites in FCC lattice.

1.7.2 Types of Spinel Ferrites

Generally spinel ferrites can be classified into three different categories due to the distribution of cations on tetrahedral (A) and octahedral (B) sites.

(1) Normal spinel ferrites

(2) Inverse spinel ferrites

(3) Mixed spinel ferrites

1.7.2.1 Normal Spinel Ferrites

In normal spinel ferrites there is present a single kind of cations on octahedral (B) sites. In normal spinel ferrites the divalent cations reside in tetrahedral (A) sites whereas the trivalent cations are on octahedral (B) sites. In normal spinel square brackets are used to specify the octahedral (B) sites to indicate the ionic distribution. Normal spinel can be expressed with the help of the formula $(M^{2+})_A[Me^{3+}]_B O_4$. Where M corresponds to

divalent ions and Me for trivalent ions. A common example of normal spinel ferrite is bulk $ZnFe_2O_4$ [10].

1.7.2.2 Inverse Spinel Ferrites

In inverse spinel structure half of the trivalent ions occupy tetrahedral (A) and half octahedral (B) sites, the remaining cations being randomly distributed among the octahedral (B) sites. These ferrites can be represented with the formula $(Me^{3+})_A[M^{+2}Me^{3+}]_B O_4$. A common example of inverse spinel ferrite is Fe_3O_4 in which divalent cations of Fe reside in the octahedral (B) sites [11].

1.7.2.3 Mixed Spinel Ferrites

Intermediate spinel ferrites are those spinel ferrites for which the distribution of ions is mixed between inverse and normal ferrites. Mixed spinel ferrites are also known as Intermediate spinel ferrites. Mixed spinel ferrites are represented with formula $(M_\delta^{2+}Me_{1-\delta}^{3+})_A[M_{1-\delta}^{2+}Me_{1+\delta}^{3+}]_B O_4$. Where δ shows the inversion parameter. Quantity δ depends on the nature of the constituents and method of preparation of the ferrites. Range of δ is between two extreme values, e.g. $\delta=1$ for normal ferrites and $\delta=0$ for complete inverse spinel. The spinel is called mixed, if there is uneven number of each type of cations on octahedral sites, examples of mixed spinel ferrites are $MgFe_2O_4$ and $MnFe_2O_4$ [11].

1.8 Applications of Ferrites

Soft ferrites are significant magnetic materials due to the constructive magnetic properties. They have extensive applications in many technologies, mostly at high frequencies[12]. There are different application for ferrites, permanent magnetic applications, entertainment applications, transformers and inductors at high power, magnetic recording, microwave applications e.g., ferrites are used extensively due to their

following features, origin of magnetic moments, high frequency application, high coercivity in selective ferrites, magnetic order, mechanical stiffness, useful temperature and time stability, wide selection of materials, high frequency applications, magneto optical properties, dielectric properties.

Ferrites can be used in electromagnetic cores containing nickel; zinc or manganese compounds can also be used in transformer. They have many applications and used in computer memories and high frequency transformer cores, Computer hard disks, floppy disks, credit card and video cassettes are some of very common soft ferrites devices [8, 12].

The existing magnetic recording technology is based on the discs and tapes, the reading and writing process are relatively easy to understand. They are essentially the same in video, audio and computer recording hard ferrites nano-particles are those which are highly resistant to becoming demagnetized a necessary characteristic for a permanent magnet.

Hard ferrites are generally used in many applications such as generator, relay, motors, loud speakers, telephones etc. Hard ferrites are the most commonly used magnets in radios.

A fastidious application requiring soft ferrites that has rapidly grown in significance in the last few years is power supplies for computers, peripherals and small instruments. An efficient and compact power unit can be obtained by using a technique known as SMPS (switch mode power supply). It may seem strange that in this technique, involving Dc to Dc conversion, one of the main elements is a high frequency transformer. In the switch mod technique, the main power signal is smooth and rectified.

In display monitors, TV deflection yokes are used to focus electrons through the interaction with strong magnetic field and generate an image on screen. The requirements for yoke of the ferrite element are related to those for high frequency transformers while the image resolution has a direct relation with the frequency needed in the horizontal scanning.

Magnetic ceramics are used in many applications such as, magnetic printers, radar-signals absorbers magnetic levitation, lithiated materials for ionic conductivity.

Magnetic fluids can be used as high-density solution for the sink-and-float separation of solids in the suspension [13].

Ferromagnetic nano-composites having magnetic nano-crystalline particles surrounded by a polymeric matrix can replace conservative ferrites in the near future for applications such as high frequency inductors, filters, core-shaped planar transformers, choke sensors, hybrid circuits and transponders.

Ferrites are also being used nowadays in television, radio, microwave, satellite-communication, automobiles, bubble devices, video, audio and digital recording. Many familiar applications associated with magnetic nano-particles are in ferro-fluids. Basically ferro-fluid is magnetic fluid made up of small magnetic nano-particles (mean diameter of 12 nm) dispersed in a carrier liquid [14,15]. There are thousands applications of magnetic nano-particles. The most familiar application is using ferro-fluids in dampening devices.

For example, overheating of the voice coils of loud speakers often damaged them because they oscillate between the poles of a circular magnet. Heat produced by the voice coil is transmitted with an increased cooling rate (factor of 3) due to filling of ferro-fluids in the gap of the permanent magnets of loud speakers [16]. Ferro-fluids can also be used in inertia dampeners such as stepper motors where these ferro-fluids serve to provide torque, opposing the stepper motor to prevent "ringing" [16]. Recently ferro-fluids are started to be used in optical applications such as optical switches and shutters though there is a lot of room for improvement. In the fields of biology and biomedicine, ferro-fluids have also established a place for their application.

Magnetic resonance imaging (MRI) is an influential technique that is used to visualize the human body based on the principles of nuclear magnetic resonance [17]. Magnetic resonance imaging (MRI) is actually the result of the difference in signal intensity that each tissue generates in response to a radio frequency pulse.

1.9 Magnetic Domain

The internal magnetic moments in ferromagnetic material can be induced by a small external magnetic field even with earth's magnetic field. Such amazing property is due to the existence of a small magnetic region called magnetic domain. Magnetic

domain is defined as "Small region in the ferromagnetic material in which all the magnetic moments are aligned in one direction".

1.9.1 Multi-Domain

Bulk magnetic material consists of groups of sub-magnetic domains, and therefore is multi-domain. Weiss suggested that magnetic moments of each individual magnetic domain align within the domain when there is no applied magnetic field, but magnetic moments of adjacent domains are not aligned. When magnetic field is applied in any direction, magnetic moments of adjacent domain align in the same direction in the presence of even a weak external magnetic field [18]. Figure 1.4 (a-b) demonstrates the magnetic domain structure in the absence and presence of applied magnetic field.
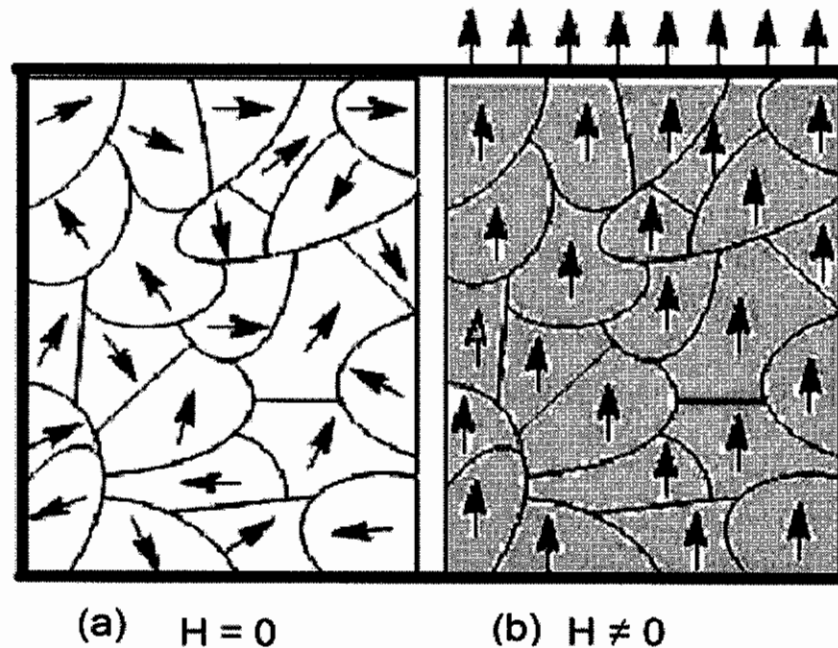
Fig. 1.4 Effect of (a) absence and (b) of magnetic field on the alignment of multi-domain material.

Microscopic confirmation indicates that alignment of magnetic moment may arise due to the domain wall movement but does not arise due to simple alignment of magnetic moments in each domain. In presence of applied magnetic field, domain walls are shifted in favor of domain with magnetic moment in parallel with applied magnetic moment as demonstrated in Fig. 1.5 [19].
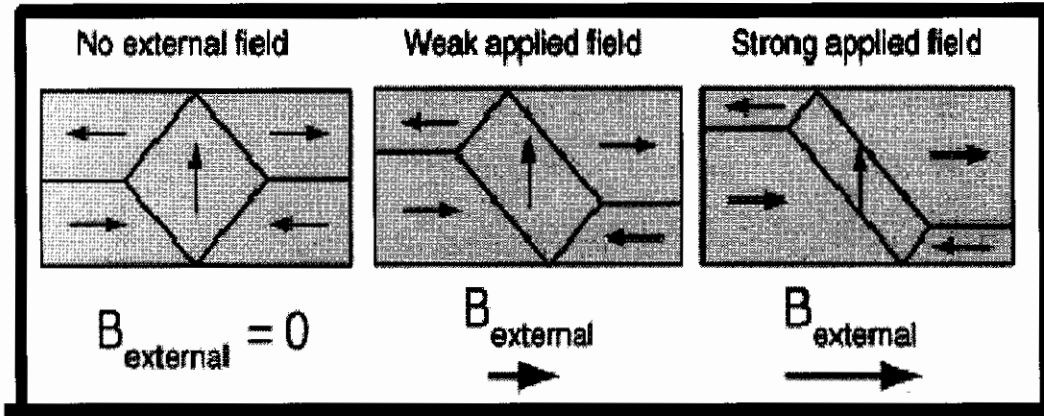
Fig. 1.5 Alignment of multi-domain and wall movement.

1.9.2 <u>Single-Domain</u>

When the grain size decreases, the materials reach a single-domain state [20]. Magnetization of a single-domain is uniform and is its saturation magnetization. It is not easy process to change magnetization of a single-domain particle and the only way to change magnetization of single-domain particle is to rotate the magnetization [21].

Therefore, a single-domain grain is magnetically hard and a multi-domain material is magnetically soft. Also a single-domain grain has large values of coercivity and remanant magnetization, where as a multi domain material has small values of remnant magnetization and coercivity [22].

1.10   Stoner-Wohlfarth Model

A magnetic medium consists of small particles and have much higher coercivity than that of a continuous medium with inclusions. Stoner and Wohlfarth had proposed a model to investigate this case with the help of an ellipsoidal particle [23].

The Stoner-Wohlfarth model is generally used for the magnetization of single-domain ferromagnetism as shown in Fig. 1.6. It is useful for modeling small magnetic particles in magnetic storage, rock magnetism and diamagnetism. The Stoner-Wohlfarth is a very simple example of magnetic hysteresis and it is the model of coherent rotation of magnetization. This makes the supposition that the directions of magnetization of all moments within the system are parallel having only two degrees of freedom.
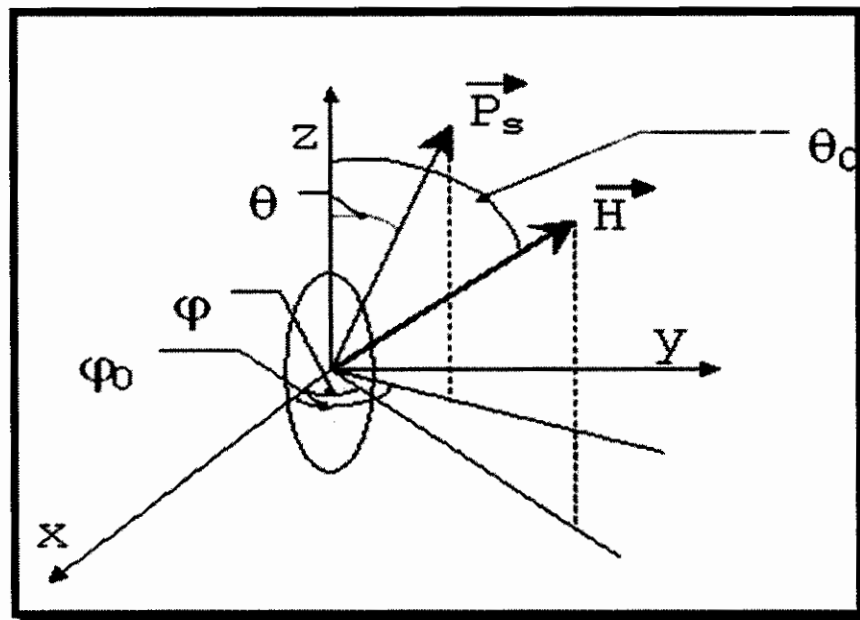
Fig. 1.6 The Stoner-Wohlfarth particle [24].

$$E = KV \sin^2(\theta - \Phi)\mu H \cos\Phi \ldots\ldots\ldots\ldots\ldots\ldots\ldots\ldots\ldots\ldots\ldots\ldots\ldots (1.11)$$

Where 'Θ' indicates the angle between the external applied field and the easy axis, 'K' represents the anisotropy energy density, 'μ' represents the magnetic moment, 'V' represents volume of a particle, 'Φ' represents the direction of the magnetic. In above

equation, the first term indicates the anisotropy energy while the 2nd term indicates the "Zeeman energy". From energy minimization, it is found that the barrier against reversal disappear when H_{ap}, reaches the value of the so called anisotropy field (H_A).

$$H_A = 2K \ / \ M_s \dots\dots\dots\dots\dots\dots\dots\dots\dots\dots\dots\dots\dots\dots(1.12)$$

By definition, H_A is the field necessary to align the moments along a field applied normal to z. This model is useful for low dimension systems with large contribution to anisotropy [25]. The Stoner-Wohlfarth model is suitable for single-domain particle behavior.

CHAPTER – 2

Experimental Techniques

2.1   Introduction

The most successful method to determine the crystal structure of material is called X-ray diffraction. Diffraction techniques can recognize chemical compounds by their crystalline structure and not from their compositions of chemical elements. It implies that the variety of compounds (or phases) that have the identical composition can be recognized. Diffraction techniques include X-ray diffraction, neutron diffraction and electron diffraction. This process was discovered in 1912 [26]. To study the properties and structure of solids, there are various experimental techniques that can be used easily. Every material possesses some chemical and physical properties. Some specific techniques are required to inspect different properties of ferrite nano-particles. Furthermore, each technique provides different specific information, some about physical and chemical properties, and other about morphology, structure and geometry.

The structure of the system and other structural parameters such as density, lattice constant and porosity were calculated from X-ray diffraction measurement. The short explanation of these techniques is given in this section.

2.2   X-ray Diffraction (XRD)

Discovery of X-rays guided toward the development of lots of major characterization instruments. X-ray diffraction is a multipurpose, non-destructive technique that gives complete information regarding the crystallographic structure and chemical composition of natural and manufactured materials. A crystal lattice is a regular 3-D arrangement (cubic, rhombic, etc.) of atoms in space. These are distributed in such a way that they form a series of parallel planes separated from one

another by an inter-planer spacing (d) which differs according to the nature of the material. For every crystal, the planes are present in a number of different orientations each with its own specific d-spacing. A crystal has an ordered 3-D periodic arrangement of atoms (molecules or ions) so the atomic planes in any crystal can be related to the unit cell.

X-rays are electromagnetic radiations with wavelength in the range of 0.5 Å to 2.5 Å. This wavelength range is comparable with inter planer distance (d) in the solid [27]. The d-spacing of lattice planes depends on how to determine the position of the peaks and size of the unit cell. Shape of the peaks and the line width may be obtained from the conditions of measurement and properties, like particle size of the sample material. The intensity of each peak is due to the crystallographic structure, i.e. their thermal vibration and the position of the atoms within the unit cell. Deceleration of fast moving electrons in the metal target and the inelastic excitation of the core electrons in the atoms of target are two ways by which we can generate the X-rays. The first process gives broad continuous spectrum while the second gives the characteristic X-rays [28].

2.2.1 <u>Bragg's Law</u>

When X-rays hits on a powder sample, the layers of crystals of the sample behave like mirrors that reflect the X-ray beam. When X-ray beams reflect off from different rows of atoms in a crystal, then Interference occurs between them. Constructive interference happens when the path difference $2d\sin\theta$ for the reflected rays becomes equal to $n\lambda$, where λ is the wavelength and n is a number.

$$2d\sin\theta = n\lambda \dots\dots\dots\dots\dots\dots\dots\dots\dots\dots\dots\dots (2.1)$$

Where   (n = 1, 2, 3...)

The Bragg's law is mostly used to analyze X-ray diffraction data. The diffraction condition is n λ =2dsinθ where θ is the angle of diffraction, d is the inter-atomic distance and is λ is the wavelength of the incident X-ray beam. The schematic representation for Bragg's Law is shown in Fig. 2.1.
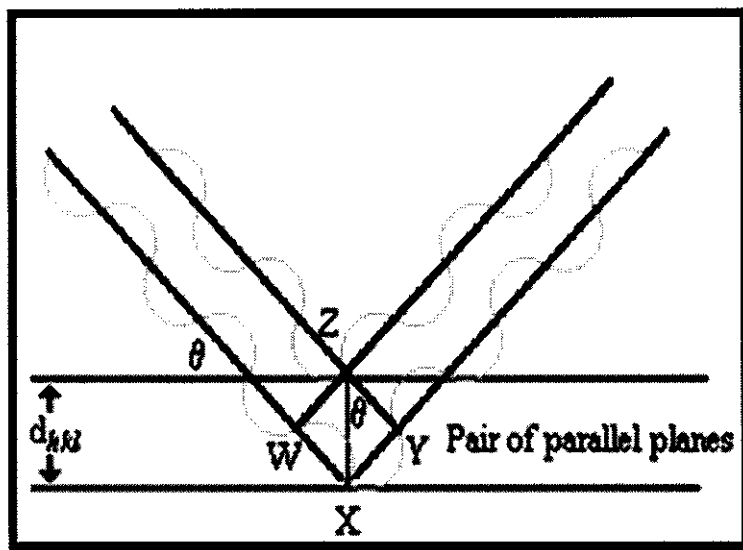
Fig. 2.1 Interference of scattered X-rays from atoms in a crystal.

Phase purity, phase identification and crystallite size can be calculated with the help of data collected from XRD. Typical wavelength range used for X-ray experiments fall between 0.6 Å and 1.9 Å. In X-ray analysis of 3-D crystal structures, following techniques are used,

1.   Rotating Crystal method

2.   Laue method

3.   Powder method

2.2.2 Powder Method

In powder technique, the incident monochromatic radiations strike a fine-grained polycrystalline specimen or powdered specimen. When diffraction takes place from a given plane (h k l), all those crystallite having (h k l) planes make an

angle θ with X-ray beam, will diffract generating a cone of constructive interference that intersect the screen in circle. Following are two techniques, which can be used for collecting data from powder diffraction method, are,

(1)   Diffractometer method.

(2)   Debye-Scherrer camera method

2.2.3 Diffractometer Method

It is the most proficient way for high-resolution data analysis. A monochromatic X-ray beam is allowed to fall on very fine powdered specimen. As all planes are present in the specimen thus for a given wavelength λ the diffraction from a plane (h k l) takes place at an angle. X-ray detector picks up this diffracted beam. Bragg designed first diffractometer in 1912 for crystallography [27].

XRD machine working in Department of physics COMSAT University, Islamabad was used for the verification of the average size of the particles and the crystal structure. In this experiment the sample was used in powdered form; the powder was positioned on the flat strip and placed in the hole (20 x 18 mm^2) of the aluminum sample holder (35x50 wmm^2, t=1.5 mm^2). The X-ray radiations used are CuK$_\alpha$ (λ = 1.5406 Å). The monochromatic X-ray beam CuK$_\alpha$ (λ = 1.5406 Å) is produced at a point and the intensities of the diffracted beam are identified with a counter. The X-ray patterns were recorded by changing 2θ from 20° to 80°.

2.2.4 Particle Size Determination

X-ray diffraction patterns were analyzed for all the samples to determine the particle size. Debye-Scherrer formula was used to calculate the particle size by utilizing the full width at half maximum (FWHM) value for the most intense peak (311) [29].

$$t = 0.9\lambda / \beta \cos\theta ....(2.2)$$

Where θ is the diffraction angle, λ is the wave length of incident X-ray (λ=1.5406 Å) and β is the full width at half maximum at θ in radians. Debye-

Scherrer formula assumed approximation and present the particle size if the particle size distribution is narrow and strain induced effects are rather negligible [30].

2.3 Electron Microscopy

X-ray diffraction (XRD) can characterize the lattice parameters and crystal structure. One of the main limitations of X-ray diffraction (XRD) is that it does not direct image the materials. Electron microscopy is complimentary to X-ray diffraction (XRD) in this sense and therefore a useful technique in this work.

In principle, electron microscopy is very analogous to optical microscopy. The key difference comes from the very short wavelength of electron beams, about 0.05 Å, which are 5 orders of magnitude smaller as compared to ordinary light. Hence we see a surprising increase of resolution and thus we can expand our ability to probe and Image small structures.

In electron microscopy, electron beam is typically emitted by a thermionic filament or an electron-tunneling source. The movement of beam is then controlled by an electric field, so these electrons acquire kinetic energy and short wavelength. The beam also passes through a series of electromagnetic lenses to focus the beam in a small size. The interaction between the beam and specimen emits electrons and photons from which required structural information can be calculated. There are two kinds of electron microscopy normally used in nanotechnology: Transmission electron microscopy (TEM) and Scanning electron microscopy (SEM). The main difference between these two techniques is the configuration of the imaging beam. For a SEM system backscattered electrons and secondary electrons are collected by the imaging sensors positioned on the same side of the electron source. In the TEM set up, the electrons pass through a thin slice of samples and the microscope works with transmitted and scattered electrons [31].

2.3.1 <u>Scanning Electron Microscopy (SEM)</u>

Scanning electron microscope (SEM) is the most extensively used form of electron microscope. It observes microscopic structure by scanning the surface of materials, similar to scanning confocal microscopes (SCM) but with much greater depth of field and much higher resolution. An SEM image is produced with the help of a focused electron beam that scans over the surface area of a sample; it is not produced by instant illumination of an entire field as for a Transmission Electron Microscopy (TEM) Probably the most significant characteristic of an (SEM) is the 3-D appearance of its images due to its great depth of field.

In SEM, the electrons emitted from the sample surface are collected and amplified with the help of a detector. The change information of secondary and back scatted electrons during scanning process is converted to the contrast in the SEM image and the topography of sample can be seen with fine detail. This is particularly useful in studying surfaces morphology, crystalline structure, chemical composition and orientation of materials making up the specimen. The image information and resolution falls between the optical and transmission electron microscopy (TEM) techniques. It is very popular instrument in laboratories due to the quite simple specimen preparation.

The surface of the scanning electron microscope (SEM) specimen should be grounded and conducting to avoid the distortion, as electrons are susceptible to the electric field generated by static charges. A thin metallic coating will help to remove the charging effect, if a specimen with insulated surface needs to be tested with high resolution.

Scanning electron microscope contains filament, an electron gun, condenser lenses, objective lens and apertures as shown in Fig. 2.2. In scanning electron microscopy, beam of electron is typically ejected from an electron gun. These electrons are accelerated by a high electric voltage between the anode and filament the two "condenser lenses" decrease the cross over diameter of the beam of electron, after that the objective lens focuses the beam of electron as a probe with a diameter

on the nm scale. The objective lens can be considered as the 3rd condenser lens in the scanning electron microscopy as it functions more like. A schematic diagram of SEM apparatus is shown in Fig. 2.2.
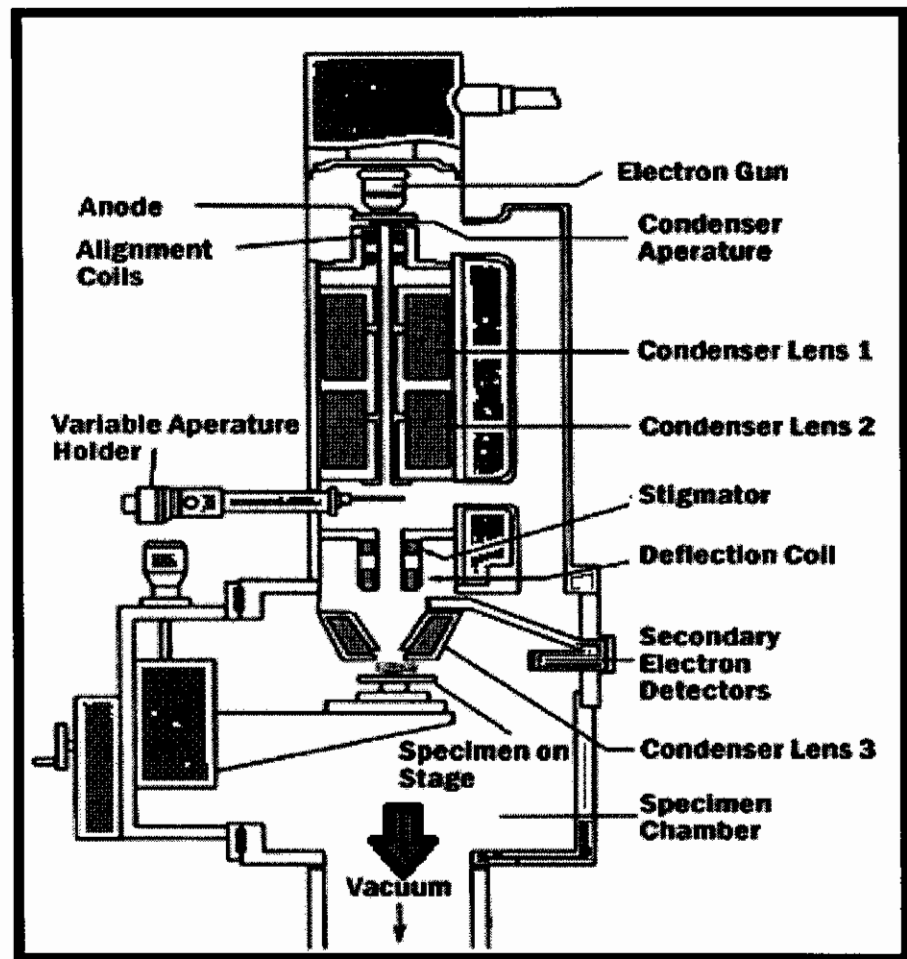
Fig. 2.2 SEM anatomy [32].

Accelerated electrons in a scanning electron microscope (SEM) have large amounts of kinetic energy and this kinetic energy is degenerated as a variety of signals due to electron- specimen interactions when the incident electrons are decelerated in the solid specimen. These signals consist of backscattered electrons (BSE), secondary electrons (that construct SEM images), diffracted backscattered

electrons (EBSD that are used to find out orientations of minerals and crystal structures), photons (characteristic X-rays that are used for continuum X-rays and elemental analysis), heat and visible light. Backscattered electrons and secondary electrons are generally used for imaging specimen: backscattered electrons are very important for illustrating contrasts in composition in multiphase specimen, while secondary electrons are much important for illustrating topography and morphology on specimen. X-ray generation is due to the inelastic collisions of the electrons in discrete shells of atoms in the specimen with incident electrons. When the excited electrons go back to the lower energy states, they give rise to X-rays that are of a specific wavelength. Therefore, characteristic X-rays are generated for each element in a mineral that is excited by the electron beam.

Scanning electron microscope (SEM) analysis is supposed to be non-destructive; that is, X-rays produced by electron interactions do not lead to volume loss of the sample, so repeated analysis of same material become possible easily.

2.4 Fourier transforms Infrared (FTIR) Spectroscopy

Fourier transforms infrared (FTIR) spectroscopy is the very famous vibrational spectroscopic technique. FTIR spectroscopy is an infrared spectroscopy where in the infrared spectrum with whole range of wave numbers is obtained by Fourier transform technique. This spectroscopic technique is different from the dispersive technique that requires the creation of a spectrum by collecting signals at each wave number independently. Presently, dispersive method has been replaced by FTIR Since FTIR has a greater value of signal-to-noise ratio than that for dispersive method.

In solid materials atoms vibrate about their mean positions. These vibrations depend on what types of atoms are there, how they are linked to other nearby atoms and how they are far from one another so these vibrations are characteristics of the solid materials. Several physical properties of materials depend on these vibrations. FTIR spectroscopy is a characterization method in which infrared radiation is passed

through the sample and a part of radiation absorbed by the sample is recorded by comparing the reference light with the light passing through sample. The FTIR method can be used for quantitative and qualitative measurements by absorption through the sample. Some part of the IR radiation is transmitted through the sample and some of it is absorbed by the sample. Both the reference and the transmitted beams are combined together. A spectrum is produced by combining these beams, which represents the molecular absorption; thus IR spectroscopy is useful for recognizing unknown material, determining the amount of a compound in a mixture and quality of a sample.

An IR spectrum gives detail of internal bond structure of constituents of a sample with absorption peaks that correspond to the frequencies of vibrations of these atoms. No two compounds can ever produce the identical IR spectrum due to their associated polarizability and different bonding nature. In this way, IR spectroscopy can result in a positive identification and qualitative analysis of materials of different kinds. A schematic diagram of FTIR apparatus is shown in Fig. 2.3.
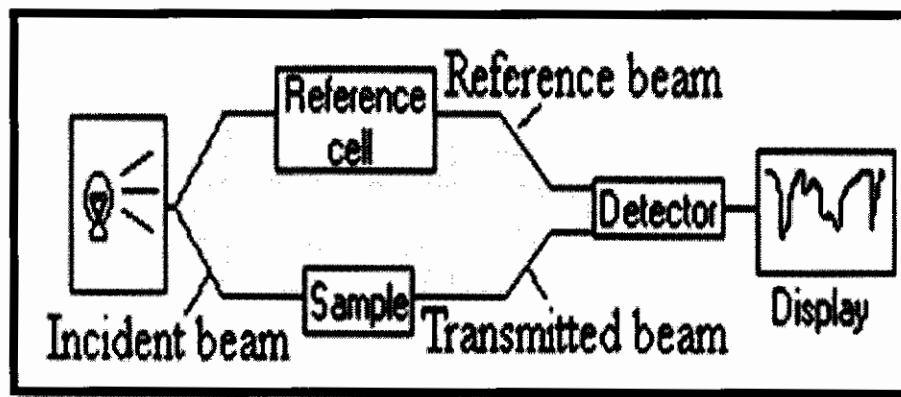
Fig. 2.3 Schematic diagram of FTIR setup

The source produce an infrared radiation and amount of energy sent to the system is controlled by the aperture. The heart of any FTIR spectrometer is a Michelson interferometer which consists of a moving mirror, a fixed mirror and a beam splitter, as shown in Fig. 2.4.

2.4.1 <u>Working Principles of Michelson Interferometer</u>

The Michelson interferometer is the main component of the FTIR system as shown in Fig. 2.4. The IR radiations from the source enter the Michelson interferometer. The interferometer is consists of two mirrors and single beam-splitter. Half of the IR beam from the source is transmitted by the beam splitter while the 2nd half is being reflected. These splited beams hit a fixed mirror and then a moving mirror. After being reflected from these mirrors, these splited beams merge at the beam splitter again to irradiate the sample before the beams are reached the detector.

2.4.2 <u>Beam-Splitter</u>

Beam splitters must be made of such material which is semi transparent to infrared light. One half portion of infrared light should be reflected to the moving mirror by the beam splitters while the rest half portion should be transmitted to the fixed mirror. The sandwich structure is most common beam splitter, in which a thin layer of germanium (Ge) is sandwiched between two layers of "potassium bromide" (KBr); it operates very well in the wave number range.

2.4.3 <u>Infrared Detector</u>

The infrared detector is such an instrument that is used to calculate the energy of infrared light from the sample to be examined. It operates as a transducer to change infrared light signals to electric signals. Two major kinds of the detector are thermal detector and the semiconductor detector [26]. A sample absorbs some of the IR radiations at characteristic frequencies according to its structure and bond strength. Atomic masses may be affected by the absorbed IR radiations. IR technique should only be used with materials whose lattice vibrations lead to alter the dipole

moment of the molecules in the sample. Otherwise, the IR is considered to be inactive because sample will not absorb IR radiations.
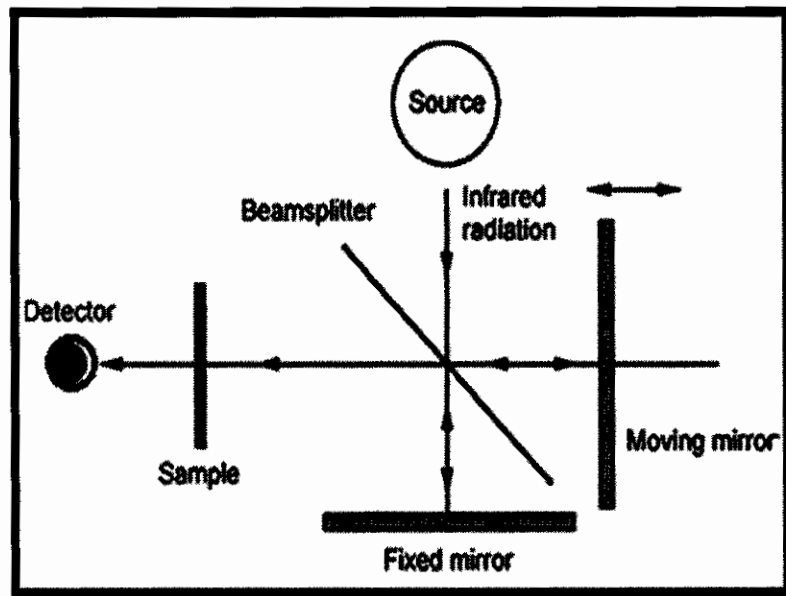
Fig. 2.4 Schematic diagram of Michelson interferometer.

For final measurements, the transmitted part of the beam enters a detector. The detectors are specially designed to measure the interferogram signal. Finally at the end, a computer programme processes the data from the detector. With the help of Fourier transform method, the computer breaks down the interferogram into its sinusoidal components, which are afterward used to calculate the absorbance values in the spectrum. The final absorbance data is then presented graphically to the user for analysis. Finally the background spectrum has been taken with KBr and sample spectrum is taken by subtracting background from the sample spectrum.

2.4.4. Procedure

1. The background spectrum was obtained by placing KBr pellet in the path of the beams with 100 scans.

2. The pellet for the sample spectrum was made by carefully mixing 5 mg of Zn-Mg ferrites sample with 50 mg of KBr and the sample spectrum was obtained with one hundred scans.

3. After the subtraction of the background, the FTIR spectrum of that sample was displayed on the computer screen.

4. The spectral resolution was 2 cm^{-1} in FTIR measurements.

5. The spectra were analyzed by using Essential FTIR software.

2.5 Vibrating Sample Magnetometer (VSM)

Vibrating sample magnetometer (VSM) was developed by S. Foner and V. Osterhart in 1956. A transducer drives the specimen to vibrate with a frequency (ω) perpendicular to the direction of applied magnetic field (H). The entire flux through the pickup coils can be written as [33],

$$F = AH + BM \sin(\omega t)..(2.3)$$

Faraday's law is the basic principle behind the vibrating-sample magnetometer (VSM). According to the Faraday's laws of electromagnetic induction, a voltage is induced in the electrical pick up circuit which is proportional to the rate of change of flux and hence to the moment within the specimen due to the applied magnetic field dt,

$$emf = -\frac{d\phi}{dt} = -BM \cos(\omega t)............................. (2.4)$$

On other way Faraday's law can also be defined as "whenever there is a change in flux linking the coil, an emf will be produced in that coil. Mathematically it can be written as,

$$v = -na\frac{dB}{dt} ....(2.5)$$

If the coil is placed in a region where magnetic field is constant, one have,

$$B = \mu_o H... (2.6)$$

When we bring a specimen having a magnetization M into the coil, we have,

$$B = \mu_o \left(H + M \right) \dots\dots\dots\dots\dots\dots\dots\dots\dots\dots\dots\dots \ (2.7)$$

The corresponding flux value can be written as,

$$\Delta B = \mu_o M \dots\dots\dots\dots\dots\dots\dots\dots\dots\dots\dots\dots\dots \ (2.8)$$

From above equations we can write as,

$$vdt = -na\mu_o M \dots\dots\dots\dots\dots\dots\dots\dots\dots\dots\dots\dots\dots(2.9)$$

This implies that the output signal of the coil is proportional to the magnetization M but does not depend on the magnetic field in which the size of magnetization is to be determined. The specimen is making to move to a sinusoidal motion (the corresponding voltage and frequency are produced in suitably positioned stationary pickup coils). The electrical output signal of these latter coils has the equal frequency and its intensity is proportional to the magnetic moment of the sample, the frequency and the vibration amplitude. A basic schematic representation of the VSM is given in Fig. 2.5.
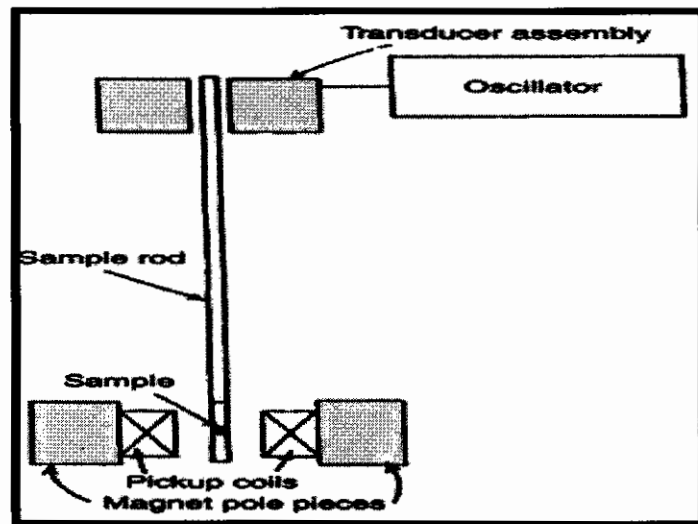
Fig 2.5 Schematic diagram of the VSM [23].

The specimen to be examined is centered in the area between the poles of a laboratory magnet, capable of producing the measuring field. A thin vertical sample rod connects the transducer assembly positioned above the magnet with the sample holder. That transducer change a sinusoidal ac drive signal generated by an amplifier circuit into a sinusoidal vertical vibration of the specimen rod. The specimen is thus subjected to a sinusoidal motion in the uniform magnetic field. So, as the specimen is vibrating near a detection coil; an AC signal is produced at the same frequency of vibration, which permits sensitive lock-in measurement to find out the magnetic moment M. The pickup coils are positioned between the pole pieces around the sample. The system is calibrated with a nickel specimen whose saturation magnetization is well recognized. In order to find out the magnetic moment M, the signal produced by the sample under observation is compared with signal produced by nickel standard. A VSM system is capable of measuring the magnetic properties of materials as a function of magnetic field, time; and temperature. Vibrating sample magnetometer (VSM) is the well-known technique for hysteresis loop measurements.

CHAPTER – 3

Synthesis of Ferrite Nano-particles

3.1 Literature survey

The characterization and properties of ferrites have been investigated due to their wide spread use and technological applications. The properties of ferrites are being upgraded due to the future trend and potential applications in ferrite technology. The results of recent studies of a few of them have been explained below.

Ferrites are well-known for a variety of properties that had no equivalents in existing metal magnetic materials. Nowadays ferrites are utilized in a truly extensive variety of applications and have contributed significantly to progress in field of electronics. Latest products having high performance appearing one after another and it seems we have only scratched the surface of the hidden possibilities of these charming materials.

The crystal structure of a ferrite can be considered as an interpenetrating of negatively charged divalent oxygen ions and positively charged metal ions. Ferrites contain metal oxides having iron oxides as their major component. The spinel ferrites commonly known as cubic ferrites are the most widely used ferrites. These ferrites belong to a significant class of magnetic materials. MFe_2O_4 is the chemical composition of a spinel ferrite. Where M is divalent metal ion such as, as Mg^{2+}, Zn^{2+}, Co^{2+}, Cu^{2+}, Fe^{2+} and Ni^{2+} etc

The development and research on ferrites received a much enhancement in recent years due to the availability of sophisticated and new methods for the production, characterization and application of nano-particles. Magnetic properties of magnetic particles can largely modify by changing particle size, which might be a useful way to design new magnetic materials. Because of large number of atoms that occupy the grain boundary area, the magnetic nano-particles have different properties as compared to bulk. Zinc ferrite nano-crystals of Ferromagnetic at ambient temperature were synthesized using the thermal decomposition of metal-surfactant complexes. Characterization of Zinc

ferrite ($ZnFe_2O_4$) particles shows that magnetic properties are particle size dependent [34].

Joshi *et. al.* [35] have been synthesized the $Zn_{1-x}Mg_xFe_2O_4$ at temperature above 1100°C and observed saturation magnetization in the range 21 to 58 emu/g. Ladgaonkar *et. al.* [36] have been synthesized the $Zn_{1-x}Mg_xFe_2O_4$ at temperature 1000°C and sintered for 24 hrs by using standard ceramic method and observed lattice parameter 8.35A°. Mazen *et. al.* [37] have been synthesized the $Zn_{1-x}Mg_xFe_2O_4$ at temperature above 1000°C and obtained lattice parameter 8.41 A°.

John Philip *et. al.* [38] studied the variations in the, average particle size, magnetic properties and crystal structure of $ZnFe_2O_4$ nano-particles on thermal annealing .using in situ high temperature XRD. Co-precipitation technique was used in these studies for preparation fine powder of $ZnFe_2O_4$ nano-particles with 9.3 nm average particle size. Under vacuum within steps of 100 °C, powder was heated from room temperature to 1000 °C and the XRD pattern is recorded in situ. It was observed that the decrease in the" lattice parameter "(a) from 8.478 to 8.468 Å at 800 °C, above which it increased with temperature. It was also observed that after sintering at 1000 °C, the lattice parameter decreased from 8.441 to 8.399 Å and the magnetization value increased from (5 to 62 emu/g). After the thermal annealing at 1000 °C, it was also noticed that the increase in the average particle size was from 9 to 27 nm.

Yahya *et. al.* [39] prepared $Zn_{1-x}Mg_xFe_2O_4$ (where x = 0.2, 0.3, 0.4 and 0.5) samples by a conventional method and pre-sintered at 1250°C and sintered at 1350 °C for 10 h in air. The value of saturation magnetization rises from 0.974 – 3.652 emu/g and then decreases to 2.508 and 1.598 emu/g.

Average particle size, variations in the crystal structure of $ZnFe_2O_4$ nano-particles and $MgFe_2O_4$ nano-particle were synthesized using the conventional double sintering technique by Abbasher *et. al.* [40].The values of the "lattice parameters" for the samples $ZnFe_2O_4$ (x =1.0) and $MgFe_2O_4$ (x =0) were found to be 8.450 Å and 8.378 Å respectively .The large value of the lattice parameter (a) for $ZnFe_2O_4$ compared to $MgFe_2O_4$ is due to the bigger ionic radius of Zn^{2+} as compared to Mg^{2+}.

S. Khot *et. al.* [41] studied $Zn_{1-x}Mg_xFe_2O_4$ (where x= 0.3- 0.6) synthesis by co-precipitation method and characterized by XRD and FTIR, SEM. The lattice parameter was obtained in the range 8.42 Å to 8.45 Å using the XRD. The lattice parameter is found to be decrease at (x=0.6) which may be ascribed to shift on some Fe^{3+} ions from (A) site to (B) site for higher composition [42]. Value of magnetization M increases by increasing value of H. The sample of x=0.4 shows the highest magnetization value and the basic composition shows the lowest magnetization value. It was observed that saturation magnetization increased first until x=0.3 and x=0.4, and then saturation magnetization decreased with the further increase in x. The saturation magnetization was associated with grain size. The smaller grain size and greater saturation magnetization was also observed at composition x=0.4.

3.2 Synthesis of Nano-particles

It has been a challenge for many researchers to synthesize nano-particles with narrow particle size distribution. The procedure of selecting raw materials depends on how much critical the properties are required. Different techniques have been adopted to obtain desirable microstructure, a small particle size and a narrow particle size distribution. Among these techniques some are dry methods or solid state methods in which the ingredient of products are mixed together directly and then given high temperature treatment. These techniques are commonly used to prepare bulk materials.

Solid precursors are frequently use for synthesis of ferrites in powdered form. However, solid-state reactions are often slow and difficult to complete unless performed at high temperatures mostly above 1100 °C. At high temperature reacting atoms can diffuse through solid materials to the reaction font easily [43].

The others are chemical methods or wet methods. In these methods, aqueous solutions of the constituent salts are mixed together. These solutions are then dried and powders are obtained

3.2.1 Chemical Methods

There is major role of chemistry in producing novel materials with new significant properties. Chemical method for preparation is well-known for its versatility in synthesizing and designing novel materials that can be developed into the final product. The basic advantage that chemical methods offer over other methods is excellent homogeneity of cation distribution, as chemical synthesis offers mixing at the molecular level. Novel materials can be prepared by designing molecular chemistry. A fundamental knowledge of phase equilibrium, thermodynamics, reaction kinetics and the principles of crystal chemistry are significant to avail many benefits that chemical processing has to offer.

Chemical methods have many advantages but on the other hand, there are also particular problems in chemical processing. In some synthesis, the chemistry is hazardous and complex. Contamination can occur due to the side reactions happening in the chemical method or from byproducts being generated. Final product with the desirable properties can be achieved by either minimizing or avoiding the effect of contamination. Agglomerations can occur at any step during the synthetic process and it can drastically change the properties of the materials [42].

For the synthesis of fine particles, precipitation of a solid from a solution is a general method. The general method involves reactions in non-aqueous or aqueous solutions having the suspended or soluble salts. The precipitate is prepared by either heterogeneous or homogeneous nucleation, when the solution gets supersaturated with the product. The formation of nuclei generally proceeds by diffusion in which reaction temperature and concentration gradient are very significant in calculating the size and the growth rate of the particles, e.g. to form mono-dispersed particles.

All the nuclei must form at almost the same time in order to produce unagglomerated particles with much narrow size distribution. For this purpose consequent growth should occur without further agglomeration or nucleation of the particles [44].

It is concluded that many factors like crystal structure, crystallinity and particle size are affected by reaction kinetics [42, 45].

Due to advantages over the conventional solid state reaction method, recently special focus has been placed on unconventional methods for obtaining fine ferrite nano-particles, through chemical methods. The particle size is a very significant parameter that has a key role in determining the subsequent electric, magnetic and optical properties of ferrite nano-particles [46]. Chemical methods have many advantages over the solid state reaction method. Due to this reason special focus has been placed on other unconventional process to obtain the ferrites nano-particle. There are different chemical methods for preparation of ferrites; few of them are given below,

- Co-precipitation method
- Reverse micelles method
- Mechanical alloying
- Micro emulsion technique
- Citrate precursor technique
- Hydrothermal method
- Sol-gel method
- Co-spray-roasting method

Co-precipitation method was employed successfully for obtaining Zn-Mg ferrite particles that have nano-metric dimensions. In addition, chemical co-precipitation method is economical method to produce ultra fine particles [47]. The co-precipitation synthesis requires neither sophisticated process nor very high processing temperature.

3.3 Influence of Different Parameters on Synthesis

Some parameters that influence the synthesis and properties of Mg-Zn ferrites are given below.

3.3.1 Influence of Temperature

For formation of ferrites the activation energy is different for different metals. Activation energy for different ferrites particles in the temperature range of $20 - 100\ ^oC$ decreases in the following manner.

EA (Ni ferrite) > EA (Co ferrite) > EA (Zn ferrite)

3.3.2 Role of Anions

In the co-precipitation solution, kinds of anions affect the properties separate for different metals. Precipitation of individual hydroxides of Zn and Fe (III) provides more pure hydroxides in the following sequence of anions: $SO_4^{-2} \rightarrow Cl^{-2} \rightarrow NO_3^{-2}$ [45].

3.3.3 Rate of Mixing of Reagents

The role of rate of mixing of reagents is very important for obtaining the desired particle size. Co-precipitation depends upon subsequent growth of particles and nucleation. For the situation where the rate of nucleation is high and the rate of particles growth is low then colloid is formed which is less dispersed in size [45].

If addition of chemical reagents in the co-precipitation reaction is slow; then the larger nuclei is formed. So to obtain smaller size ferrite particles, the mixing of chemical reagent should be very fast [48].

3.4.4 <u>Influence of pH of the Reaction</u>

When the pH of reaction is made to increase from 6.8 to 8.6 then yield of ferrites in case of Zn ferrites also grows. Rise of pH value from 8.6 to 10 gives only minor growth in the yield. A significant increase in the yield is observed when the pH value is increased from 12.5 to 14 [45]. pH range required for the formation of the Zn-Mg ferrite particles is nearly 12.5.

3.3.5 <u>Duration of Heating after Co-Precipitation</u>

Co-precipitation occurs in a concentrated system, but no information is provided on particles size growth, which may happen in such a system during long heating process. Mg-Zn ferrites nano-particles solution was heated for 45 min. after formation of precipitates.

3.4 Explanation of Apparatus used for the Synthesis

Following apparatus was used for the synthesis of different samples of Mg-Zn spinel ferrite nano-particles.
Digital electronic Balance

- pH Meter
- Stirring Machine
- Mortar and Pestle
- Furnace
- Crucibles
- Oven

3.4.1 Digital Electronic Balance

A digital electronic balance having accuracy of $\pm$ 0.001 g was used for weighing materials. Care should be taken to set the balance for zero setting before each measurement.

3.4.2 pH Meter

pH meter with temperature sensor was used for accurate measurement of pH value and temperature of the solution. The pH meter has accuracy (± 0.01 pH) and pH range from 0.00 to 14.00. The temperature sensor has accuracy of $\pm$ 0.5°C and it measuring range is from 0 to 100 °C.

3.4.3 Stirring Machine

We used the magnetic stirrer with hot plate for homogeneous mixing and heating the solution. The hot plate can supply the temperature from room temperature to 370 °C.

3.4.4 Pestle and Mortar

Pestle and Mortar were used for grinding purpose. The material of the Pestle and Mortar should be very hard otherwise there are chances of mixing of its element with sample materials. The Pestle and Mortar used was made of agate.
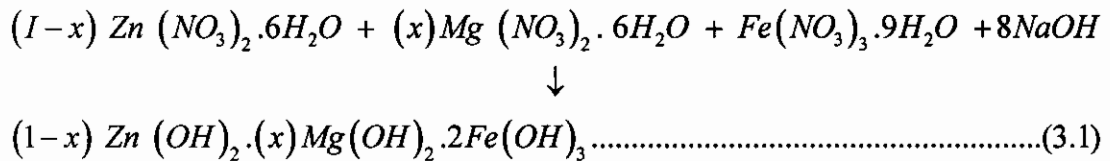
3.4.5 Crucibles

Boat type crucibles were used for heating purpose. Boat type crucibles used were made of porcelain material having melting point above 1500 °C. To dry the sample materials an oven that can provide temperature range from room temperature to 250 °C

was used. An electric furnace was used in experimental work for sintering of different type of samples. The maximum attainable temperature by this furnace is 1400 °C.
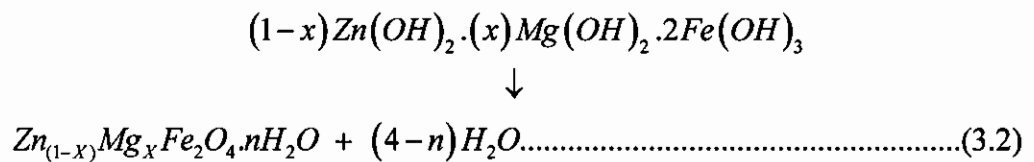
3.5   Synthesis of $Zn_{1-x}Mg_xFe_2O_4$ Nano-particles

The, structural, magnetic and electrical properties of spinel ferrite nano-particles are found to depend on the grain size and the process of synthesis. Chemical co-precipitation is comparatively easy to scale up and also widely used to synthesize ferrites nano-particles. Co-precipitation is used to synthesize ferrites such as Mn-Zn ferrites, Co-Zn ferrites, Co-Ni ferrites, Ni-Zn ferrites, etc. Fine particles of ferrites are obtained with the co-precipitation from aqueous solution of divalent M^{2+} and trivalent Fe^{3+} where Co^{2+}, Fe^{2+}, Zn^{2+} and Ni^{2+} may serve as M^{2+}. The initial molar proportion (M^{2+}/Fe^{3+}) is always considered as the stoichiometric 0.5. The co-precipitation reaction takes place in two stages [45].

At initial stage, solid hydroxides of metals in the form of colloidal particles are obtained by the co-precipitation of metal cations in alkaline medium. For Zn-Mg ferrites this reaction occurs as

$$(1-x)\ Zn\ (NO_3)_2 .6H_2O\ +\ (x)Mg\ (NO_3)_2 .\ 6H_2O\ +\ Fe(NO_3)_3 .9H_2O\ +8NaOH$$
$$\downarrow$$
$$(1-x)\ Zn\ (OH)_2 .(x)Mg(OH)_2 .2Fe(OH)_3 \dots\dots\dots\dots\dots\dots\dots\dots\dots\dots\dots\dots\dots(3.1)$$

In next stage, product is subjected to heat in the precipitation alkaline solution to provide the transformation of solid solution of metal hydroxides to the Zn-Mg ferrites,

$$(1-x)Zn(OH)_2 .(x)Mg(OH)_2 .2Fe(OH)_3$$
$$\downarrow$$
$$Zn_{(1-x)}Mg_xFe_2O_4 .nH_2O\ +\ (4-n)H_2O \dots\dots\dots\dots\dots\dots\dots\dots\dots\dots\dots\dots(3.2)$$

In above equation n is an integer. The main feature of the co-precipitation method is that the product is heated in alkaline solution for many hours but a particular amount of water is still associated with it [45].

Ferrites nano-particle of composition $Zn_{1-x}Mg_xFe_2O_4$ with x varies from 0.0 to 0.5 was prepared by co-precipitating technique. The chemical reagents used in this experiment were ferric nitrate (hydrated) $Fe(NO_3)_3.9H_2O$, zinc nitrate (hydrated) $Zn(NO_3)_2.6H_2O$, and "magnesium nitrate" (hydrated) $Mg(NO_3)_2.6H_2O$. All these chemical reagents were of analytical grade and used without more purification. The aqueous solutions of the chemicals $Zn(NO_3)_2.6H_2O$, $Mg(NO_3)_2.6H_2O$ and $Fe(NO_3)_3.9H_2O$ were mixed in NaOH. The molarity value of the co-precipitation agent NaOH utilized was 50 ml of 1.5 M in distilled water.

Solutions of $Zn(NO_3)_2.6H_2O$, $Mg(NO_3)_2.6H_2O$ and $Fe(NO_3)_3.9H_2O$ in their stoichiometry 50ml of 0.24 M $Zn(NO_3)_2.6H_2O$, 50 ml of 0.16 M $Mg(NO_3)_2.6H_2O$ and also 50 ml of 0.8M $Fe(NO_3)_3.9H_2O$ in the case of $Zn_{0.6}Mg_{0.4}Fe_2O_4$ and in the same way for the other values of x were dissolved in distilled water under constant stirring, unless a clear solution was obtained. To obtain ferrite nano-particles which are less dispersed in size, smaller size and more chemically homogeneous, the mixing of reagents was carried out very quickly by adding the precipitating reagent NaOH rapidly into metal solutions, contained in a beaker, with constant stirring till co-precipitation occurred. It was required to keep the solution for 45 minutes at a temperature of 70 °C for the transformation of hydroxides into ferrites. The stirring speed was tried to keep constant for all values of Mg concentration. The pH value of the reactions was also tried to maintain between '12.5-13'. Distilled water was used to clean the precipitates until these precipitates were free from chloride and sodium ions. Electric oven was used to dry the product at a temperature of 100 °C for 12 h to remove water content. After that the dried powder was mixed homogeneously in mortar and agate for 25 minutes; Acetone was used initially and at the end of process for cleaning the pestle and mortar [45].

$$Mass = Volume \times mol.wt. \times Molarity / 1000 \text{.....................(3.3)}$$

The samples were cooled gradually to room temperature. Synthesis steps of that processes are also shown in Fig. 3.1.

Mg (NO₃)₂.6H₂O   H₂O   Zn (NO₃)₂.6H₂O   H₂O

+

Fe(NO₃)₃.9H₂O   H₂O

NaOH   H₂O   Stirring (30 mint)

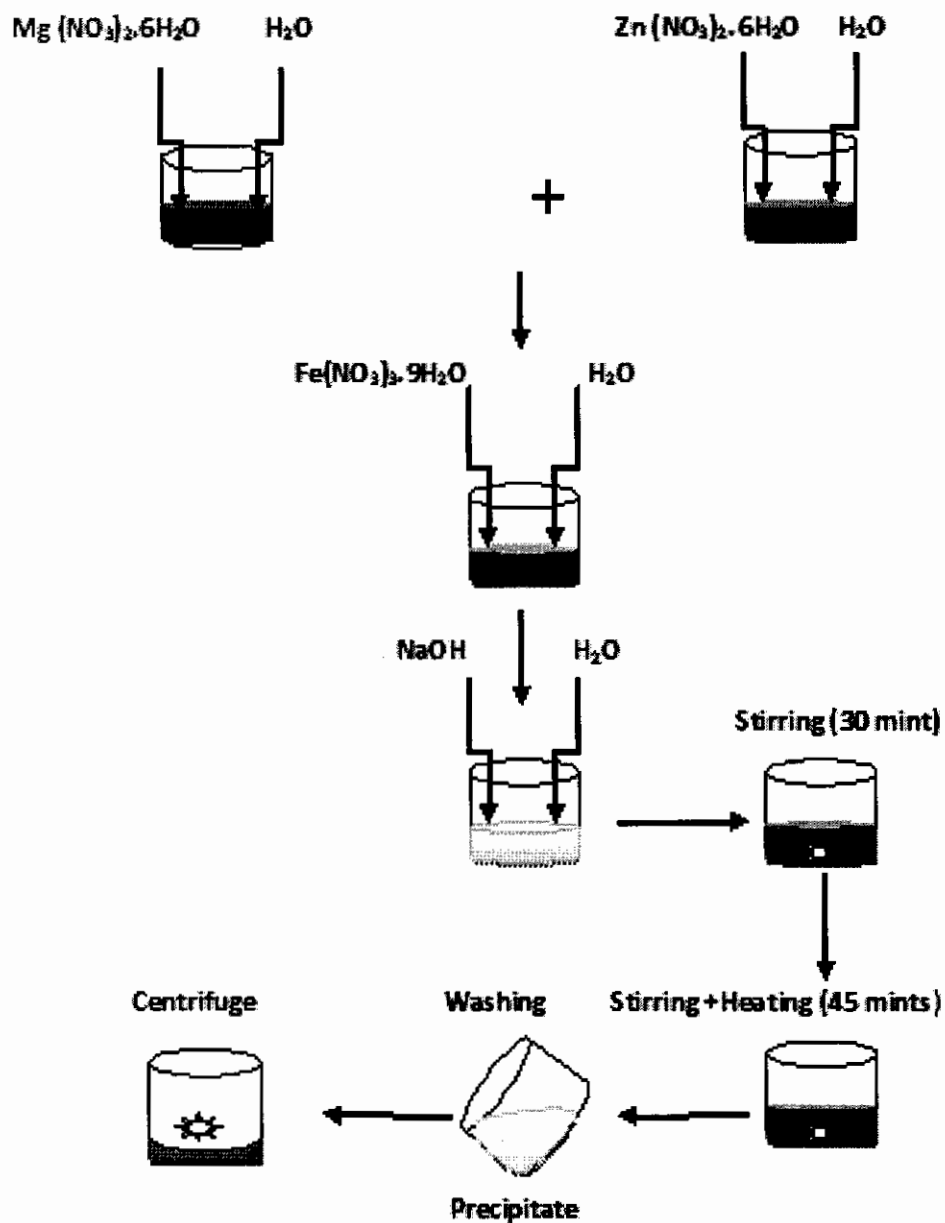Centrifuge   Washing   Stirring + Heating (45 mints)

Precipitate

Fig. 3.1 Schematic diagram of the synthesis process of $Zn_{1-x}Mg_xFe_2O_4$ by co-precipitation method

CHAPTER – 4

Results and Discussion

Soft spinel ferrites have been explored intensively for many years because of their potential applications in industry. The most popular type of soft ferrite magnetic material is the cubic spinel crystal $NiZnFe_2O_4$. Spinel ferrites have chemical formula MFe_2O_4 in which M can be any divalent metal ion. In spinel ferrite structure, oxygen forms an FCC lattice with cations at octahedral (B) and tetrahedral (A) sites [49]. The unit cell of a spinel ferrite consists of 8 divalent, 16 trivalent iron and 32 oxygen metal ions, e.g., zinc ferrite ($ZnFe_2O_4$), nickel ferrite ($NiFe_2O_4$) and cobalt ferrite ($CoFe_2O_4$). The spins at the octahedral and tetrahedral sites are anti-parallel to each other. Divalent M^{2+} and trivalent Fe^{3+} are distributed over octahedral and tetrahedral lattice sites [50]. Preference of divalent metal ion M^{2+} depends upon the type of the spinel structure e.g. normal, inverse and mixed spinel structure. In case of normal spinel structure, Fe^{3+} ions are distributed equally over both lattice sites [51]. Physical properties are strongly influenced by preference of metal ion on these lattice sites. The magnetic and structural environment of these two sites can be controlled by the chemical composition, synthesis methods, and sintering temperature. Also the concentration and type of cations substitution have very dominant effect on the physical properties. The magnesium ferrite MFe_2O_4 has a mainly inverse spinel structure with the preference of Mg^{2+} ions predominantly on octahedral sites [52]. While the zinc ferrite $ZnFe_2O_4$ has the normal spinel structure, in which the Zn^{2+} ions occupy the tetrahedral sites [53]. Both Zn and Mg divalent ions are diamagnetic in nature. Due to diamagnetic nature of Zn ions and equal distribution of Fe^{3+} ions on two lattice sites, the total magnetization of the chemical formula $ZnFe_2O_4$ is zero [54]. There is not so much literature available on the mixed system Zn-Mg ferrite which could be very interesting due to different lattice preferences of Zn and Mg ions, and very valuable soft magnet spinel ferrite which could replace the toxic Ni-Zn soft ferrite in many practical applications. In the present work, the Zn-Mg ferrite nano-particles with different composition ($Zn_{1-x}Mg_xFe_2O_4$ with x = 0.0 – 0.5) have been prepared and their physical

properties are studied in detail. Our experimental work can be divided into two parts as follows:

4.1 Structural properties (X-ray diffraction, FTIR spectroscopy, SEM).

4.2 Magnetic properties (VSM).

4.1 Structural Properties

Structural analysis includes X-ray diffraction (XRD), Fourier transform infrared (FTIR) spectroscopy and scanning electron microscopy (SEM) and discussed below in sections 4.1.1 – 4.1.3.

4.1.1 X-ray Diffraction (XRD)

X-ray diffraction is one of famous scientific technique to investigate the structural parameters and average particle size of nano-particles [54]. The initial structural characterization of $Zn_{1-x}Mg_xFe_2O_4$ ferrite nano-particles were done by using X-ray diffraction (XRD). The indexed XRD patterns of the samples are shown in Fig. 4.1.
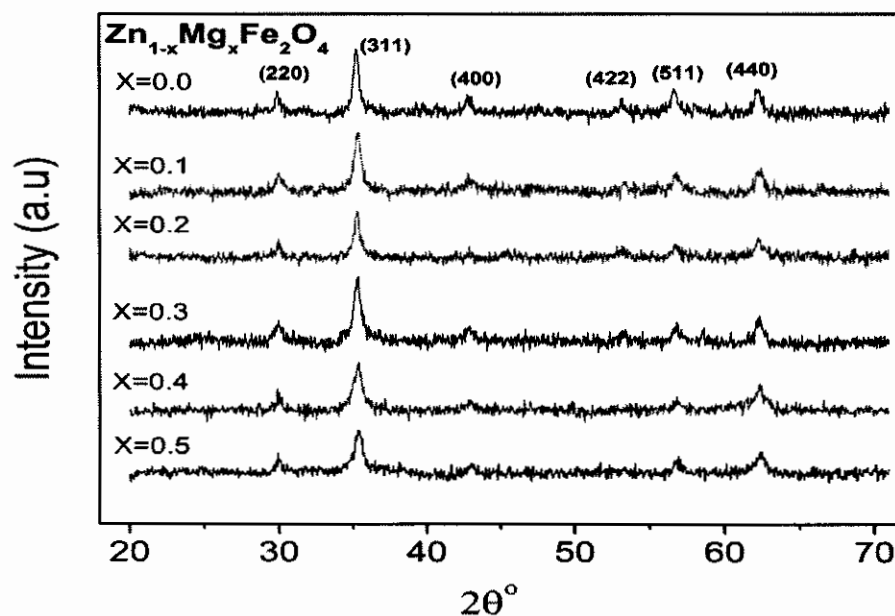

Fig. 4.1 XRD patterns of ferrite $Zn_{1-x}Mg_xFe_2O_4$ nano-particles with x = 0.0 – 0.5.

Table 4.1 Parameters calculated from XRD data of all the samples.

Mg concentration (x)	Zn-Mg ferrite	Lattice constant (Å)	Average nano-particle size (nm)
0.0	$ZnFe_2O_4$	8.4323	29
0.1	$Zn_{0.9}Mg_{0.1}Fe_2O_4$	8.4249	35
0.2	$Zn_{0.8}Mg_{0.2}Fe_2O_4$	8.4280	60
0.3	$Zn_{0.7}Mg_{0.3}Fe_2O_4$	8.4109	60
0.4	$Zn_{0.6}Mg_{0.4}Fe_2O_4$	8.4217	44
0.5	$Zn_{0.5}Mg_{0.5}Fe_2O_4$	8.4090	29

The experimental peaks of all the specimens were indexed with standard pattern JCPDS for $Zn_{1-x}Mg_xFe_2O_4$ nano-particles and broadness of the peaks suggest that the dimensions of products are in nano-scale. The average particle size was estimated considering the most intense peak (311) and using the Debye-Scherrer formula,

$$t = 0.9 \, \lambda \, / \, \beta \, \cos\theta \dots\dots\dots\dots\dots\dots\dots\dots\dots\dots\dots (4.1)$$

Where t is average particle size, θ is the diffraction angle, λ is the wavelength of incident X-ray and β is the full width half maximum of the most intense peak (311) in units of radians. Debye-Scherrer formula assumes approximation and gives the particle size if that particle size distribution is thin and strain induced effects is rather negligible [56].

All the samples were prepared under the same circumstances; the particle size remains within the range 29 – 60 nm for different compositions [40].

The particles sizes as a function of Mg concentration is listed in Table 4.1 and presented in Fig. 4.2 (a).
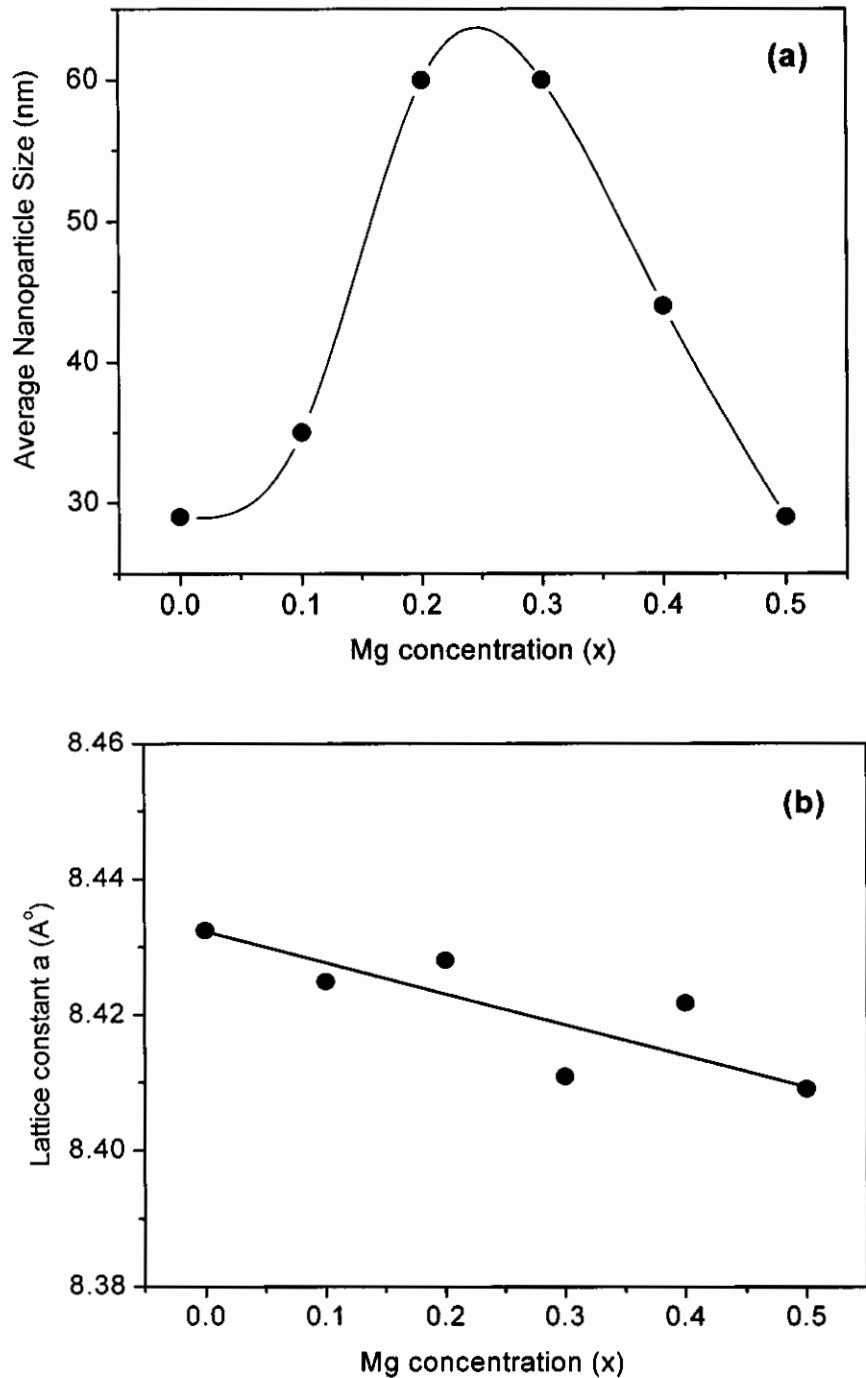
Fig. 4.2 (a) Average particle size vs. Mg concentration, (b) Lattice constant vs. Mg concentration of $Zn_{1-x}Mg_xFe_2O_4$ nano-particles with x = 0.0 − 0.5. Solid lines just show the trend.

Initially the estimated size is increasing with increasing Mg concentration up to x=0.3 and then shows a decreasing trend with further increase of Mg.

The lattice parameter 'a' was calculated using the lattice spacing'd' values and the respective miller indices (h k l) parameters. The lattice constant 'a' was calculated by using the formula given below;

$$a = d_{(hkl)} / \sqrt{h^2 + k^2 + l^2} \dots\dots\dots\dots\dots\dots\dots\dots\dots\dots (4.2)$$

The lattice parameter is found to be in the range 8.40 to 8.43 Å as shown in Fig. 4.2(b) [57, 58]. It shows a decreasing behavior with increasing Mg concentration and is attributed to smaller ionic radius of the Mg^{2+}(0.06 nm) cation as compared to Zn^{2+}(0.074 nm) cation .

4.1.2 Scanning Electron Microscopy (SEM)

Scanning electron microscope (SEM) is a versatile surface imaging techniques used to study shapes of different nano-structural as well as bulk materials [59]. The scanning electron microscopy (SEM) micrographs of all the samples $Zn_{1-x}Mg_xFe_2O_4$ at magnification 50000 are shown in Fig. 4.3(a – f), which indicate the distribution and size of nano-particles.
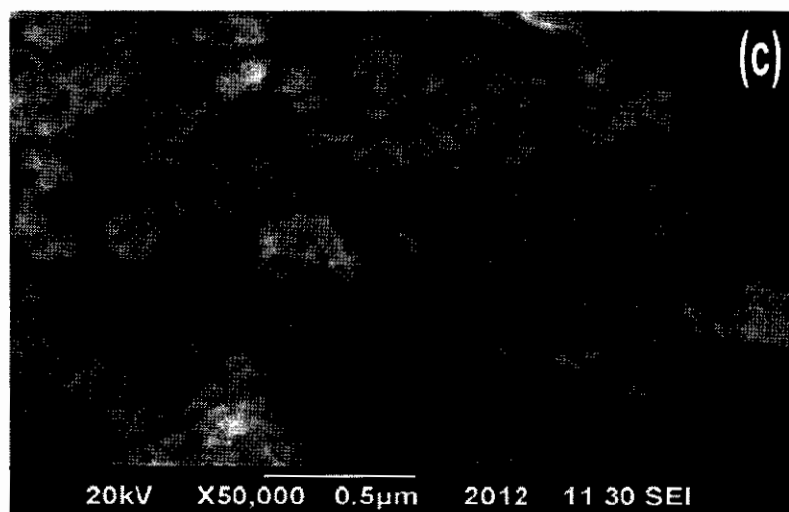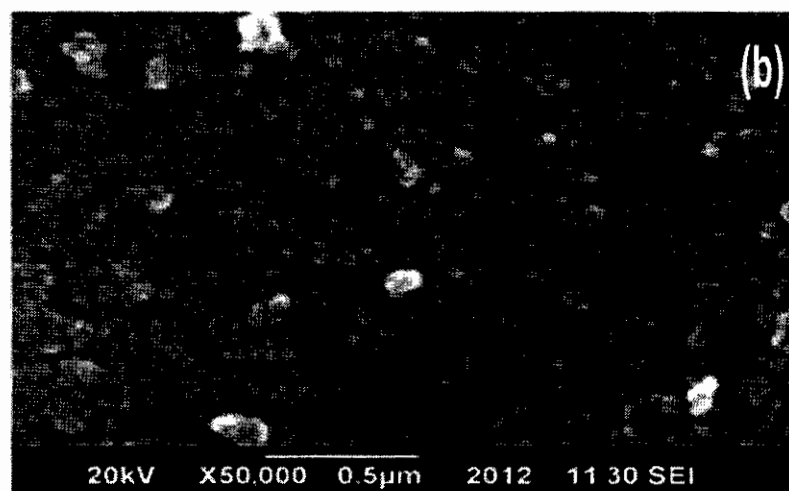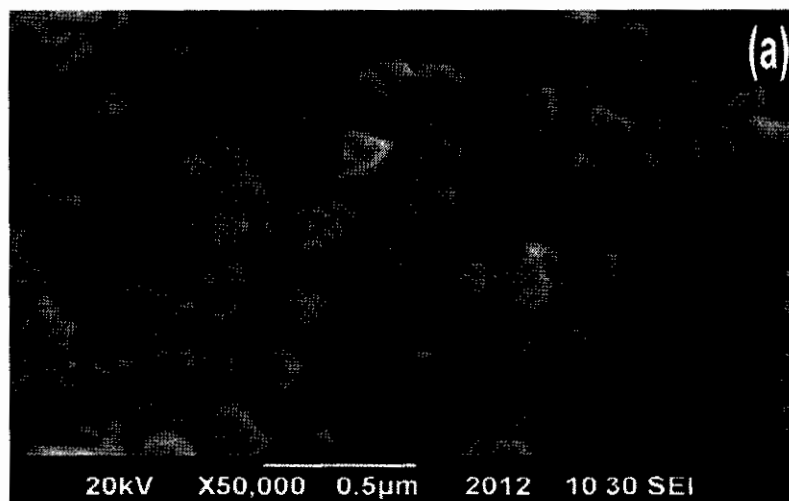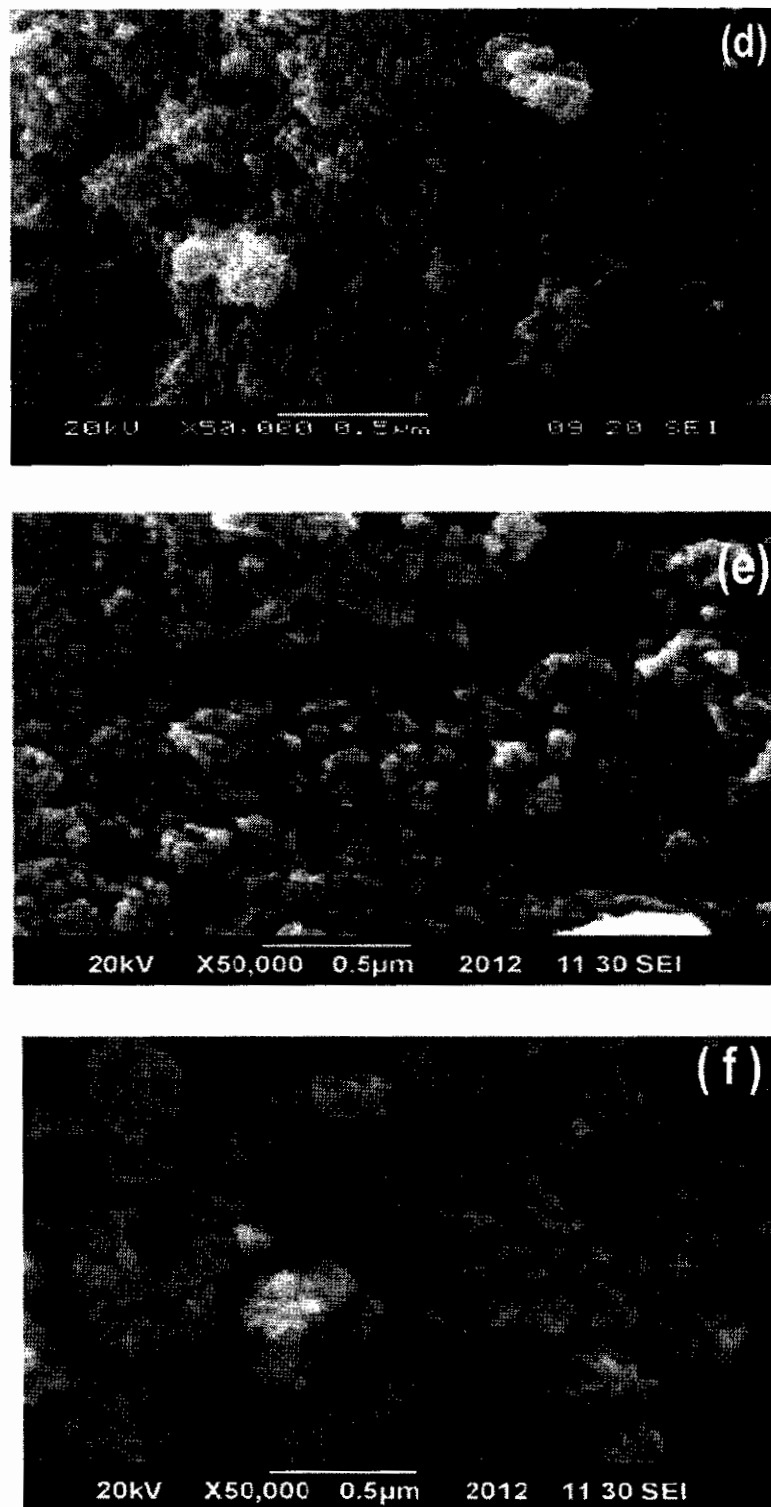
Fig. 4.3 (a – f) SEM micrographs of $Zn_{1-x}Mg_xFe_2O_4$ nano-particles with x= 0.0 – 0.5 at 50000 magnification.

4.1.3 Fourier Transform Infrared (FTIR) Spectroscopy

The formation of ferrite nano-particles has been studied by FTIR spectroscopy in the far-infrared region ($400 - 660$ cm^{-1}) and one of the samples $ZnFe_2O_4$ FTIR spectrum is shown in Fig. 4.4. The IR absorption measurements were done using the KBr pellet technique.
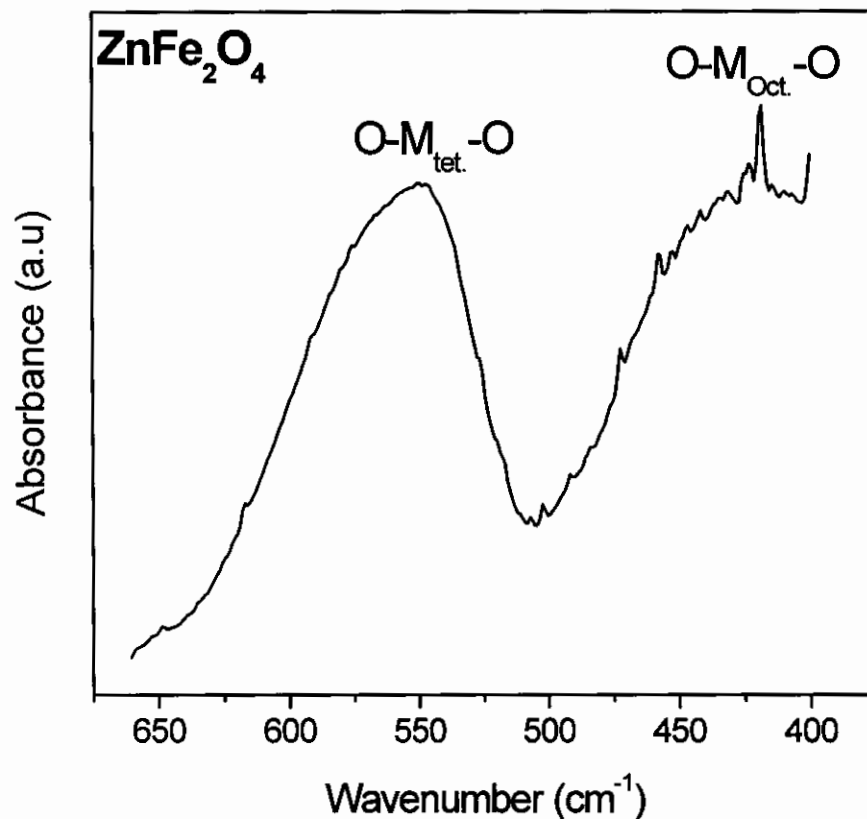
Fig. 4.4 FTIR spectrum of KBr-pelletized sample $ZnFe_2O_4$.

The band at 418 cm^{-1} is attributed to the vibration of the chemical O-$M_{Oct.}$-O bond in location of the octahedron and the band at 545 cm^{-1} is attributed to the vibration of the chemical bond O-$M_{tet.}$-O in location of the tetrahedron, respectively [60]. The presence of these absorption bands signifies the formation of ferrite spinel structure of zinc ferrite.
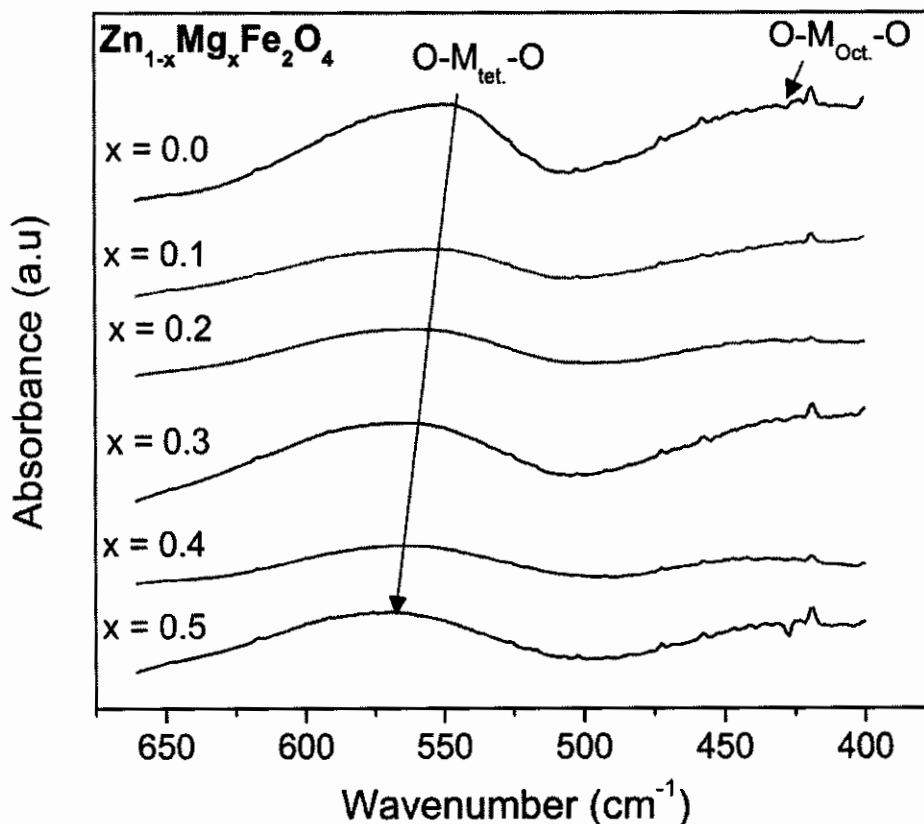
Fig. 4.5 FTIR spectra of all the samples $Zn_{1-x}Mg_xFe_2O_4$ with x = 0.0 - 0.5.

Figure 4.5 shows the far-infrared spectrum of KBr-pelletized samples $Zn_{1-x}Mg_xFe_2O_4$ with x = 0.0 – 0.5. Bands at 545 and 420 cm^{-1} correspond to tetrahedral and octahedral site coordination of metal ions with oxygen in the spinel crystal structure, respectively [61]. Arrow at O-M$_{tet.}$-O indicates the shift of vibration band with increasing Mg concentration [62].

It was observed that the O-M$_{tet.}$-O band is shifted to higher wave numbers with the increase of Mg concentration (x = 0.0, 0.1, 0.2, 0.3, 0.4 and 0.5). Pradeep *et al.* has reported shifts in the vibrations bands of Mg ferrite nano-particles on substitution of Ni, Cu and Zn ions and attributed to the change of the environment of ions in the tetrahedral and octahedral sites [63]. In our case the change in the O-M$_{tet.}$-O band is dominant and is

due to the local environmental change and change in bond lengths on doping the Zn ions [64].

4.2 Magnetic Properties

Magnetization measurements were done using a vibrating sample magnetometer (VSM) at room temperature with a maximum magnetic field of 8 kOe. As we have already discussed in Ch. 1, magnetization of the spinel ferrites nano-particles are strongly influenced by the cationic distribution on the tetrahedral and octahedral lattice sites. Magnetic moments at octahedral and tetrahedral lattice sites are anti-parallel to each other [65]. Figure 4.6 shows the MH-loop of pure Zn ferrite nano-particles at room temperature at maximum applied field of 8 kOe. Pure zinc ferrite (x = 0.0) nano-particles show a paramagnetic behavior due to its incomplete normal spinel structure [66]. The presence of hysteresis (see inset of Fig. 4.6) in Zn ferrite may be due incomplete normal spinel structure of the Zn ferrite nano-particles and/or may be due to presence of disordered surface spins [67].
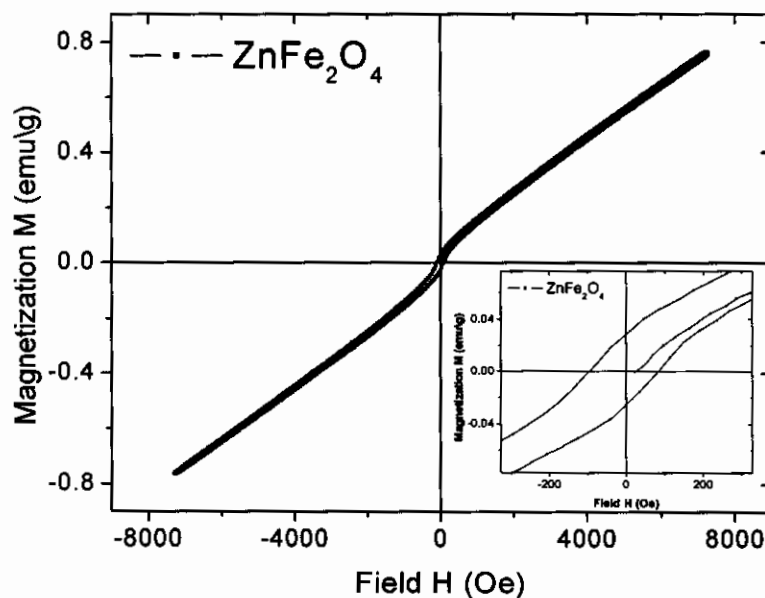

Fig. 4.6 MH-loop of pure Zinc ferrite ($ZnFe_2O_4$) nano-particles at room temperature. Inset: Coercivity region.

MH-loops of all the samples $Zn_{1-x}Mg_xFe_2O_4$ with x = 0.0 – 0.5 at room temperature are shown in Fig. 4.7. In normal spinel structure of zinc ferrite, Zn^{2+} divalent ions occupy tetrahedral sites. With the addition of Mg^{2+} divalent ions, ferromagnetic behavior increases and we got hysteresis for all the samples (x>0.0).
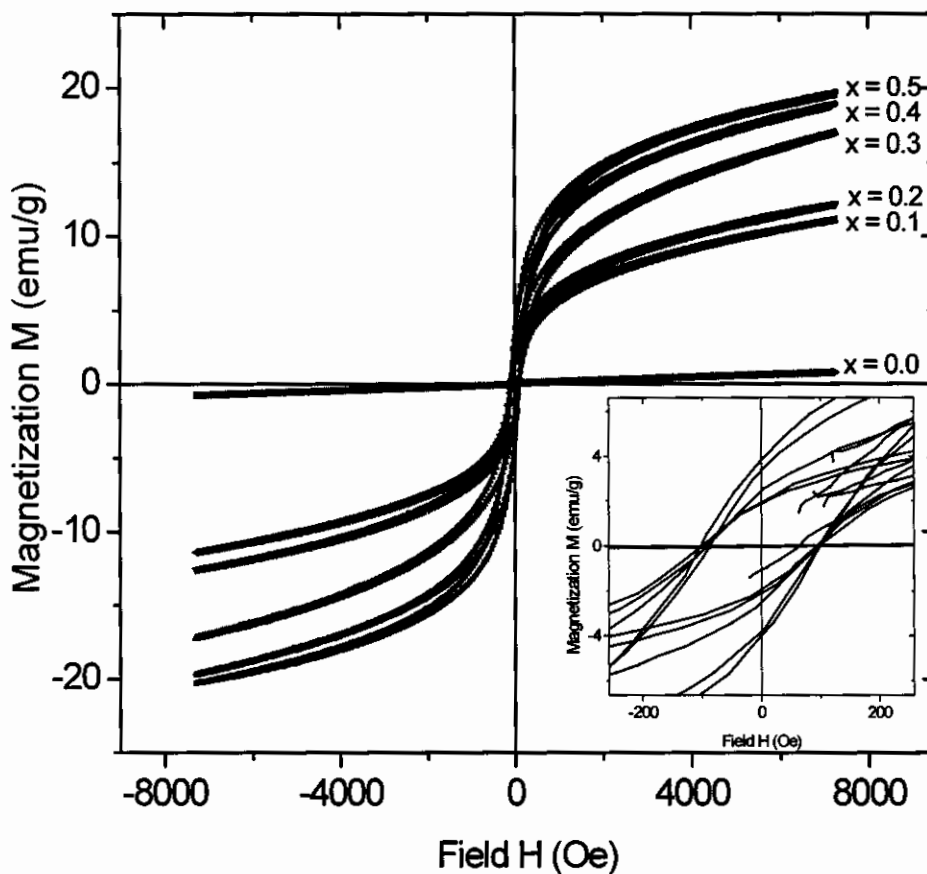

Fig. 4.7 MH-loops of the samples $Zn_{1-x}Mg_xFe_2O_4$ with x = 0.0 – 0.5. Inset shows the coercivity region.

Magnetization parameters such as coercivity (H_c) and magnetization at 8 kOe (M_{8kOe}) evaluated from Fig. 4.7 and shown in Fig. 4.8 (a, b).
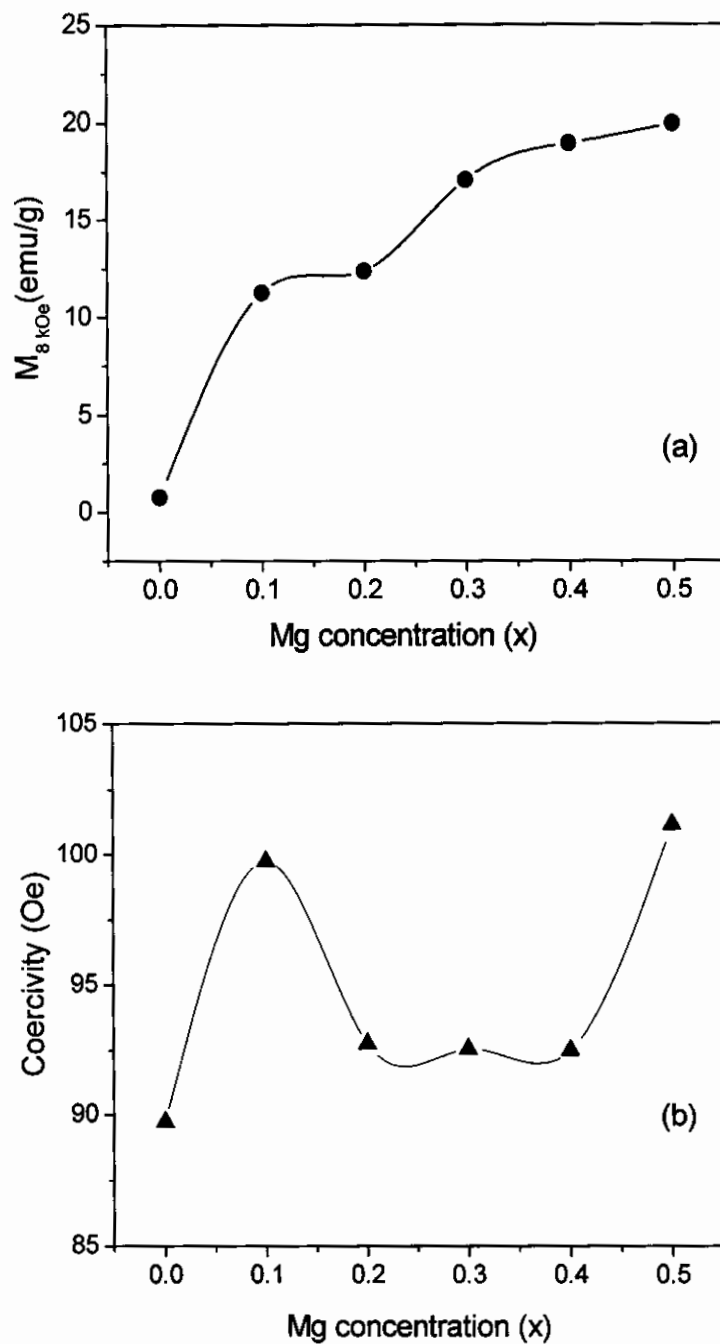
Fig. 4.8 (a) Variation of magnetization at 8 kOe versus Mg concentration, (b) Variation of

coercivity with Mg concentration.

It was expected that there will be no change in net magnetization because non-magnetic Mg ions replace non-magnetic Zn ions. But interestingly magnetization at maximum field of 8 kOe shows a monotonic increase with increasing Mg concentration as illustrated in Fig. 4.8 (a). In the literature, it is reported that the pure bulk Mg ferrite exhibits inverse spinel structure in which Mg^{2+} ions prefer octahedral sites [68]. But in nano-particles form, Mg ferrite shows magnetism which may be due to its incomplete inverse spinel structure at the nano-scale [69]. Therefore, in our case, increase in net magnetization with increasing Mg concentration is attributed to misbalance of Fe^{3+} ions on the octahedral and tetrahedral lattice sites. Misbalance of Fe^{3+} ions change the strength of superexchange interactions among the ions present at octahedral and tetrahedral sites which results in the increase in net magnetization. Although average nano-particle size is also changing with Mg concentration (see Fig. 4.2 (a)) and we get smaller particle size for samples x = 0.0 and 0.5 but the magnetization is increasing with Mg concentration (see Fig. 4.6 (a)) which demonstrate that in our samples cationic distribution is dominate over size effects or surface effects. And also the surface effects are more dominant in the nano-particles with diameter less than 20 nm which is below our particle size range (29 – 60). Kodama *et al.* [70, 71] has reported a model for magnetization (M) of fine nano-particles which shows a decrease in M with diminishes particle size due to presence of disordered surface spins. Coercivity (H_c) fluctuates in the range 90 – 100 Oe as the Mg concentration is increased from 0.0 to 0.5. Smaller values of coercivity for all the samples indicate the soft magnetic nature of these ferrite nano-particles and also the presence of ferromagnetic behavior at room temperature [72].

4.3 Conclusion

Zinc ferrite nano-particles doped with Mg ion ($Zn_{1-x}Mg_xFe_2O_4$ with x = 0.0 – 0.5) were sucessfully synthesized by co-precipitation method. Initial structural characterization was done by using XRD. Average particle size calculated by Debye Sherrer's formula lies in the range 29 – 60 nm for different compositions. It shows maximum particle size for the samples with compositions x = 0.2 and 0.3. Lattice parameter 'a' shows a decreasing trend with increasing Mg concentration and is attributed to smaller ionic radius of the Mg ion as compared to Zn ion. SEM shows that there is not so much scatter in the particle size and nano-particles are nearly spherical in shape. Specific vibrational bonds in FTIR spectroscopy confirm the formation of spinel Zn-Mg ferrite nano-particles in accordance with the XRD. FTIR results also show the shift of vibration band located at tetrahedral site with increasing Mg concentration which is attributed to change in local chemical environment and change in bond lengths. On doping the Mg ions, ferromagnetic behavior increases and shape of the MH-loops changes. Magnetization at maximum field shows a monotonic increase with increasing Mg concentration which is attributed to change in cationic distribution at the tetrahedral and octahedral sites. Smaller values of coercivity shows that the soft magnetic nature of these ferrite nano-particles.

It can be concluded that different changes in Zn-Mg ferrite nano-particles properties occur due to rearrangements of metal ions on the tetrahedral and octahedral sites in the spinel ferrite structure. Spinel ferrite Zn-Mg shows a soft magnetic behavior with enhanced magnetic properties which can be very useful for practical applications.

References

1.   http://nanogloss.com/#axzz1mkKZaYsI (2011).

2.   E. Ebad, Nano dictionary (2005).

3.   C. Q. Sun, B. K. Tay, S. Li, X.W. Sun, S.P. Lau, and T.P. Chen, Mater. Phys. Mech. **4**, 129 (2001).

4.   V. Kumar, A. Rana, M.S. Yada, and R.P. Pant, J. Magn. Magn. Mater. **320**, 1729 (2008).

5.   A. Gadkari, T. Shinde and P. Vasambekar, J. Mater. Sci.Mater. Electron. **21**, 96 (2010).

6.   www.csus.edu/indiv/n/ngw/EEE-161/wk-12/Lecture/Applied%20Magnetism.ppt.

7.   G. Blasse, J. Phys. Chem. Solids. **26**, 1969 (1965).

8.   www.ims.uconn.edu/~alpay/Courses/MMAT%20244/Lecture%2019.ppt. (16-Jul-2008).

9.   H. P. J. Wijin and J. Smit, "Ferrites", Jhon Wiley and Sons, New York, (1959).

10.   S. Son, M. Tehri, E. Carpenter, V.G. Harris, and M.E. McHenry, J. Appl. Phys. **91**, 7589 (2002).

11.   A. J. Decker, "Solid State Physics", Mc Milan Press Ltd. London (1995.

12.   C. R. Vestal and Z. J. Zhang, Chem. Mater. **14**, 3817 (2002).

13.   P. Xu, X. Han and M. Wang, J. Phys.Chem. C **111**, 5866 (2007).

14.   J. D. Livingston, "Driving Forces: The Natural Magic of Magnets", Harvard University Press: Cambridge, (1996).

15.   R.C. O' Handley, "Modern Magnetic Materials: Principles and Applications", Wiley and Sons, Inc.: New York, (2000)

16.   P. Kinnari, R. V. Upadhyay and R.V.Mehta, J. Magn. Magn. Mater. **252**. 35. (2002).

17.   A. Goldman, "Modern Ferrite Technology", Van Nostrand Reinhold, New York, (1990).

18.   S. J. Park, S.Kim, S.Lee, K.Char and T.Hyeon, J. Am. Chem. Soc. **122**, 8581 (2000).

19. C. Liu, B. Zou, A. J. Rondinone and Z. J. Zhang, J. Amer. Chem. Soc. **122**, 6263 (2000).

20. R. S. Knox, J. Am. Chem. Soc. **87**, 3288 (1965).

21. H. Kim, M. Achermann, L. P. Balet, J. A. Hollingsworth and V. I. Klimov, J. Amer. Chem. Soc. **127**, 544 (2004).

22. D. Dinega and M. G. Bawendi, Angew. Chem. Int. Ed. Engl. **38**, 1788 (1999).

23. wikipedia, http://en.wikipedia.org/wiki/Stoner%E2%80%93Wohlfarth_model

24. http://stoner.phys.uaic.ro/eimm_courses/stoner-wohlfarth.html.

25. R. S. David sellmyer, "Adv. Mag. Ultrahard magnetic Nanostructures (USA)" (2012).

26. Y. Leng, "Materials Characterization", John Wiley & Sons (2008).

27. B. D. Cullity, "Elements of X-ray Diffraction", 2nd Edition, Addision-Wesely, New York (1978).

28. K. L. Horovitz, "Solid State Physics", Academic Press, New York, (1959)

29. H. P. Klug and L. E. Alexander, "X-ray Diffraction Procedures for Polycrystalline and Amorphous Materials"; 2nd ed., John Wiley: New York, (1974).

30. I. Lisiecki, P. A. Albouy and M. P. Pileni, J. Phys. Chem. B **108**, 20050 (2004).

31. S. Wischnitzer, "Introduction to Electron Microscopy", Pergamon Press, (1981).

32. http://www.fen.bilkent.edu.tr/~aykutlu/msn/hw/Microscopy.pdf

33. B. D. Cullity, "Introduction to Magnetic Materials", Addision-Wesely, New York (1972).

34. C. Yao, G. F. Goya, T. Torres, J. Liu, H. Wu, M. Ge, Y. Zeng, Y. Wang and J. Z. Jiang, J. Phys. Chem. **111**, 12274 (2007).

35. J. H. Joshi and R. G. Kulkarni, J. Material Sci. **21**, 2138 (1986).

36. B. P. Ladgaonkar, P. N. Vasambekar and A. S. Vaingankar, J. Magn. Magn. Mater. **210**, 289 (2000).

37. S. A. Mazen, S. F. Mansour and H.M. Zaki, J. Appl. Phys. **38**, 471 (2003).

38. J. Philip, G. Gnanaprakash, G. Panneerselvam, M. P. Antony and T. Jayakumar, J. Appl. Phys. **102**, 054305 (2007).

39. A. Noorhana Yahya, A. Aziz and H. Daud, Am. J. Engg. Appl. Sci. **54** (2008).

40. A. M. Abbasher, H. M. Widatallah, A.D. Al-Rawas, M. Elzain and A.Yousif, J. Phys. Conf. **217,** 012138, (2010).

41. S. Khot, B. P. Ladgaonkar, B.Kale and S.C.Watawe, Adv. Appl. Sci. Res. **4,** 460 (2011).

42. H. S. Nalwa, "Handbook of Nanostructured Materials and Nanotechnology", Vol 1, 3-4.

43. S. Patil, S. Kadam and B. Chougule, Bull. Mater. Sci. **14,** 1225 (1991).

44. S. Son, M. Taheri, E. Carpenter, V. G. Harris and M. E. McHenry, J. Appl. Phys. **91,** 7589 (2002).

45. E. Auzans, "Mn-Zn Ferrite nanoparticles for water and hydrocarbon based ferrofluid", PhD thesis, Institute of Physics of Latvian University (1999).

46. C. Cazier and M. Stefanescu, Physica B **327,** 129 (2003)

47. V. P. Blaskov, V. Rusanov, V. Martinez, L. M. Martinez and S. Mikhov, J. Magn. Magn. Mater. **162,** 331 (1996).

48. C. Yao, Q. Zeng, G. F. Goya, T. Torres, J. Liu, H. Wu, M. Ge, Y. Zeng, Y. Wang and J. Z. Jiang, J. Phys. Chem. C **111,** 12274 (2007).

49. R. G. Kulkarni and H. H. Joshi, J. Solid State Chem. **64,** 141 (1986).

50. D. S. Joshi G, A. Khot and S. Sawant, Ind. J. Phys. **A61,** 251 (1987).

51. R. H. Kodama and A. E. Berkowitz, J. Appl. Phys. **81,** 5552 (1997).

52. R. G. Kulkarni and H. H. Joshi, Solid State Commun. **53** 1005 (1985).

53. B. P. Ladgaonkar, P. P. Bakare, S. R. Sainkar and A. S. Vaingankar, Mater. Chem. Phys. **69,** 19 (2001).

54. K. P. Thummer, M. C. Chhantbar, K. B. Modi, G. J. Baldha and H. H. Joshi, J. Magn. Magn. Mater. **280,** 23 (2004).

55. S. R. Sawant and R. N. Patil, J. Mater. Sci. **16,** 3496 (1981).

56. R. D. Waldron, Infrared Spectra of Ferrites, Phys. Rev, **99,** 1727 (1955).

57. M. A. Hiti, J. Magn. Magn. Mater. **192,** 305 (1999).

58. E. Shora and M. Hiti, Mater. Sci. Tech. **14,** 625 (1998).

59. G. Blasse, Philips res. Rep. Suppl. 3 **91,** (1964).

60. Y. Koseoglu, A. Baykal, M. S. Toprak, F. Gozuak, A. C. Basaran and B. Aktas, J. Alloys and Comp., **462** 209 (2008).

61. S. A. Patil, V. C. Mahajan, A. K. Ghatage and S. D. Lotke, Mater. Chem. Phys. **57**, 86 (1998).

62. Q. Yang, B. Han, T. Sun, L. Yan, X. Wang, Dyes and Pigments **55**, 9 (2002).

63. A. Pradeep and G. Chandrasekaran, Materials Letters, **371**, 374 (2006).

64. V. Kassabova-Zhetcheva and L. Pavlova, Cent. Eurp. J. Chem. **5**, 107 (2007).

65. H. Joshi, P. Pandya, K. Modi ,N. Jnai, G. Baldha and R. Kulkanri, Bull. Mater. Sci. **20**, 93 (1997).

66. P. Holec and J. Plocek, J. Sol-Gel Sci. Tech. **51**, 301 (2009).

67. S. W. da Silva, F. Nakagomi, M. S. Silva, A. C. Oliveira and P. C. Morais, J. Appl. Phys. **107**, 09B503 (2010).

68. W. Sun, J. Liu and G. Hu, J. Mater. Sci.-Mater. Electron. **23**, 995 (2012).

69. Q. Song and Z. J. Zhang, J. Amer. Chem. Soc. **126**, 6164 (2004).

70. R. H. Kodama, J. Magn. Magn. Mater. **200**, 359 (1999).

71. R. H. Kodama, A. E. Berkowitz and S. Fone, Phys. Rev. B **59**, 6321 (1999).

72. Z.L. Lu, L.Y. Lv, J.M. Zhu, S.D. Li, X.C. Liu, W.Q. Zou, F.M. Zhang, Y.W. Du, Solid State Commun., **137**, 528 (2006) .